Reduction of arsenate and inorganic trivalent chromium mobility in soils
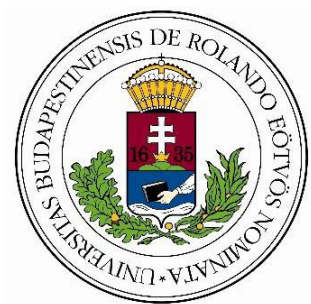
PhD dissertation

Timothy Amangdam Anemana

Supervisors: Dr. Viktor G. Mihucz associate professor

Dr. Enikő Tatár associate professor

Department of Analytical Chemistry

Eötvös Loránd University

Doctoral School of Environmental Science

Head of the School: Prof. Dr. Imre Jánosi

Environmental Chemistry Doctoral Program

Head of the Program: Prof. Dr. Tamás Turányi

Eötvös Loránd University

Cooperative Research Center for Environmental Sciences

Budapest

2020

Table of contents

List of Abbreviations

Acronym	Notion
AAs-EK	approaching anodes electrokinetic
AC	activated charcoal
AFS	atomic fluorescence spectrometry
APX	ascorbate peroxidase
As	arsenic
iAs(III)	arsenite
iAs(V)	arsenate
ATR	attenuated total reflection
BC	biochar
BCR	Community Bureau of Reference
CA	citric acid
CAT	catalase
CCA	chromated copper arsenate
c_e	equilibrium concentrations in the liquid phase
CEC	cation exchange capacity
Cr	chromium
CRM	certified reference material
DW	deionized water
EDS	energy dispersive spectroscopy
EDTA	ethylenediamine tetraacetic acid
EKR	electrokinetic remediation
EXAFS	extended X-ray absorption fine structure (spectroscopy)
FAAS	flame atomic absorption spectrometry
FTIR	Fourier-transformation infrared
GF AAS	graphite furnace atomic absorption spectrometry
GR	glutathione reductase
HA	humic acid
HF	hydrofluoric acid

HM	heavy metal
HR	high resolution
K_F	Freundlich constant
K_L	Langmuir constant
ICP	inductively coupled plasma
ICP-AES	inductively coupled plasma atomic emission spectrometry
ICP-SF-MS	inductively coupled plasma sector field mass spectrometry
LMWOA	low-molecular weight organic acid
MS	mass spectrometry
MTs	metallothioneins
MW	microwave
$NH_2OH \cdot HCl$	hydroxylamine hydrochloride
NPs	nanoparticles
nZVI@BC	nanozerovalent biochar
OA	oxalic acid
OM	organic matter
PCs	phytochelatins
PGPB	plant growth promoting bacteria
POX	peroxidase
PP	polypropylene
PSD	particle size distribution
PTFE	poli(tetrafluoreten)
PZC	point of zero charge
q_e	equilibrium concentration in the solid phase
$q_{m,L}$	maximal adsorption capacity
SC	sorption capacity
SBDC	sludge-derived biochar
SBFL	sugar beet factory lime
SEM	scanning electron microscopy
SM&T	Standards, Measurements and Testing Programme

SOD	superoxide dismutase
TCLP	toxicity characteristic leaching procedure
TMs	toxic metals
TXRF	total-reflexion X-ray flurescence
XAFS	X-ray absorption fine structure
XANES	X-ray absorption near structure
XPS	X-ray photoelectron spectroscopy
XRD	X-ray diffraction
XRF	X-ray fluorescence spectrometry

1. Research Background and Problem Statement

Chromium (Cr) and arsenic (As) contamination of natural water bodies and soil systems has caused serious environmental quality deterioration because of urbanization, industrialization and rapid population growth. Chromium and As pollution is caused by atmospheric deposition, agricultural chemical application, natural rock weathering, mineral mining, wood preservation, industrial activities among others. In particular, organoarsenic feed additives have veterinary benefits but the soluble forms of As species are excreted into the environment after arsenical compounds are administered to animals to improve development, promote growth, control parasites and enhance efficient feed utilization. These activities have caused widespread As and Cr soil contamination and destabilization of the ecosystem resulting in human health problems. Unlike in aqueous systems, removal of heavy metal (HMs)/metalloids from soils is difficult to accomplish. The best available ways are to reduce Cr(VI) to Cr(III) coupled with other mechanisms to stabilize it in the soil system. Additionally, arsenite [iAs(III)] is not only more toxic, but may represent a greater carcinogenic hazard than iAs(V). Several conventional methods have been adopted for soil remediation, which include chemical precipitation, solidification, soil washing, chemical reduction, electrokinetics, and bioremediation, etc. Oftentimes, organic materials, which are readily available, are usually employed to accomplish metal/metalloids stabilization in soil systems. Moreover, functionalization of these organic materials is promising alternative to increase the efficacy of these organic materials for metal/metalloid remediation. Activated carbon prepared from *Arachis hypogea* shell as a biowaste, available in large quantities may be a promising candidate for mobility reduction of iAs(V) in acidic sandy soil and the suitability of natural brown coal in different grain sizes for Cr(III) mobility reduction in both acidic and carbonaceous sandy soils has not been extensively elaborated.

2. Objectives

The objectives of the present thesis aimed at reduction of mobility of inorganic trivalent chromium and arsenate in soil systems. The specific objectives are listed as follows:

1. To study the reduction of inorganic Cr(III) contamination by immobilization using appropriate and inexpensive sorbent in acidic and calcareous sandy soils.

2. Determination of physico-chemical characteristics of lignite affecting Cr mobility to elucidate the Cr-lignite adsorption mechanism.

3. Assessment of Cr distribution on the water-soluble, carbonate bound and easily reducible fractions in the acidic and calcareous sandy soils as well as estimation of the phytoavailable fraction of Cr by applying appropriate leaching tests.

4. To find a cheap biowaste material readily available in large quantities, suitable for carbonization and activation by simple and cost-effective methods for mobility reduction of arsenate [iAs(V)] in acidic sandy soil.

5. Amendment of iAs(V) artificially contaminated soil with suitable activated carbon (AC) by investigating the immobilization rate.

6. Application of the carbonized and activated peanut shell biowaste material and its HNO_3, Celite® or Florisil® composites for reduction of iAs(V) mobility in acidic sandy soil.

7. To investigate the effect of oxalic acid (OA), a low-molecular weight organic acid in the enhancement of the immobilization rates as a result of further protonation of AC and iAs(V) ions by OA.

8. Elucidation of the binding mechanism of iAs(V) by the AC prepared from the peanut shell in aqueous phase and in soil.

3. Literature Overview

3.1 Arsenic and chromium contaminants in soils

Arsenic (As) is ubiquitous priority pollutant, carcinogenic and highly toxic metalloid element in the environment [1]. The oxidation states of As are from - 3 to + 5. The inorganic species such as arsenite [iAs(III); H_3AsO_3] and arsenate [iAs(V); H_3AsO_4, $H_2AsO_4^-$, $HAsO_4^{2-}$, AsO_4^{3-}]. Arsenite is more mobile and toxic than iAs(V). Arsenic speciation is governed by redox potential (Eh) and pH. Under oxidizing conditions, at low pH (pH<6.9), $H_2AsO_4^-$ dominantes while at higher pH values, $HAsO_4^{2-}$. However, H_3AsO_4 and AsO_4^{3-} species may be present in extremely acidic and alkaline conditions, respectively. At pH less than pH 9.2 under reducing conditions, the uncharged arsenite species, H_3AsO_3 predominates [2]. These conditions govern the mobility, availability, and bio-accessibility of As in the environment [3]. Arsenic pollution is caused by both geogenic release e.g. plants and microorganisms and anthropogenic activities e.g. sewage irrigation, atmospheric deposition and mine exploitation. This inevitably leads to higher risk of disastrous environmental and human health hazards such as skin and liver cancers as a result of geogenic and anthropogenic activity-induced emission sources [4, 5].

Chromium (Cr) occurrence in the environment is attributed to Cr-containing rock weathering and volcanic eruptions. Concentrations of Cr in seawater, rivers and lakes ranges from 1 and 300 mg/kg, 5 to 800 µg/L and 26 µg/L to 5.2 mg/L, respectively [6]. The most mobile forms of chromium in the soils is Cr(VI) which occurs as chromate ($HCrO_4^-$ and CrO_4^{2-}) ions. However, the reduced Cr(VI) species could form complexes with organic ligands like; NH_3, OH^-, Cl^-, F^-, CN^-, SO_4^{2-} after reduction by soil organic matter (OM) such as; S^{2-} and Fe^{2+} ions under anaerobic conditions [7]. The hazardous contamination of hexavalent chromium [Cr(VI)] originates from several activities like textile manufacturing, metal processing, wood preservation, cement production, leather tanning, mining, electroplating, steel and automobile manufacturing, paint pigments and dyes processing [8]. Chromium can be transported by surface runoff to water bodies in its soluble or precipitated form. Since the leachability of Cr(VI) increases as soil pH increases, soluble and unadsorbed Cr complexes can leach from soil into groundwater. Distribution of the polluting elements is strongly related to the soil properties and the behavior of the element [7].

Elemental pollution has prompted the WHO to reduce the maximum permissible level of As from 50 μg/L to 10 μg/L [9]. Similarly, FAO UN report on the B Status of the World's Soil Resources states that, countries with mature industrial sectors and well-developed regulatory framework must consider identification and remediation of contaminated soils as a major issue [10]. Therefore, it is imperative to consider HM soil ecosystems contamination remediation, restoration and protection measures capable of characterizing and remediating soil contaminants to ameliorate their accumulations and transfer into the food chain [9]. As a result, development of new technologies for soil remediation is of practical and scientific importance especially application of waste materials for HM and metalloid stabilization [11]. Several technologies encompassing isolation, stabilization, oxidation, physical separation and phytoextraction have been employed for metal/metalloid-contaminated soils remediation [12]. These remediation technologies utilize various stabilization mechanisms to ameliorate metal/metalloid contamination through adsorption [e.g., humic substances, Fe(III)-oxyhydroxides], complexation (e.g., humic substances, EDTA) and precipitation (e.g., phosphates) [13, 14].

3.2 Remediation technologies for arsenic and chromium contaminants in soils

3.2.1 Lime and carbonate application for metal and metalloid immobilization in soil

Soil acidification is a major point of discussion because of its influence on HM and metalloid phytoavailability in soil systems. Soil acidification can affect soil pH to influence metal/metalloid speciation, solubility, mobility and phytoavailability in the soil system [15, 16]. Toxic metals (TMs) responsible for soil contamination is a global problem adversely affecting ecosystem health and food security [17].

Application of lime [e.g., $CaCO_3$, CaO, $Ca(OH)_2$] to HM contaminated soil systems could present promising remediation potentials [18]. Similarly, materials with high potential to remediate contaminated soils is slags of calcium metasilicate (Ca_2SiO_3) and magnesium orthosilicate (Mg_2SiO_4) which differ only in their silicate content [19]. Liming for contaminated soil remediation provides various advantages like simplicity, cost effectiveness, flexibility of treatment method and recyclability of contaminated soils back to usable state [18].

Liming raises the cation adsorption and increases the net negative charge of the soil system [20]. In relation to liming, several physico-chemical processes could be employed in this context to stabilize metal contaminants by applying Friedel matrix or lime, clay, polyamine carbamates, apatite, as well as other soluble phosphates, zeolite, zerovalent iron, iron based minerals, triple superphosphate, diammonium phosphate, wet detoxification and solidification/stabilization (S/S) [21-23]. However, in limed agricultural soil, the competition of Ca^{2+} with other divalent ions on root surface is greatly enhanced [20]. Soil amendment with lime could significantly decrease the OM-bound, reducible oxide-bound and residual fraction of chromium in the soil system [18].

Regarding arsenic immobilization, lime or cement could be employed for arsenic immobilization via the formation of insoluble Ca-As compounds including; $Ca_4(OH)_2(AsO_4)_2 \times 4H_2O$, $Ca_3(AsO_4)_2$, Ca-As-O and $NaCaAsO_4 \times 7.5H_2O$ [24]. Some varieties of these liming agents include; limestone ($CaCO_3$), quick lime (CaO), slaked lime [$Ca(OH)_2$], dolomite [$CaMg(CO_3)_2$], and slag ($CaSiO_3$) with different acid-neutralizing potentials [25]. Phosphate materials such as; phosphate rock (PR), oxalic acid (OA)-activated PR, super phosphate, and bone meal could also be utilized for effective immobilization of contaminants in mine tailings [26]. When liming amendment is employed for contaminant immobilization, most of metals and metalloids are transformed into relatively stable form as a result of the higher $Ca(OH)_2$ content, which increases the alkalinity and effectiveness of the solidification process [27, 28].

3.2.2 Role of lignite and humic acids on chromium stabilization in contaminated soil

Lignite is a natural resource, it is the youngest type of coal, and widely utilized as solid fuel. Lignite contains high amounts of oxygen-containing functional groups such as carboxyl (−COOH), hydroxyl (−OH) and carbonyl (=C=O) functional groups responsible for cation exchange capacity (CEC) [29]. There are different types of coal which are grouped based on fixed carbon content, heating values and degree of coalification process. The types of coal are thus, lignite, subbituminous, bituminous and anthracite (Figure 1) [30].
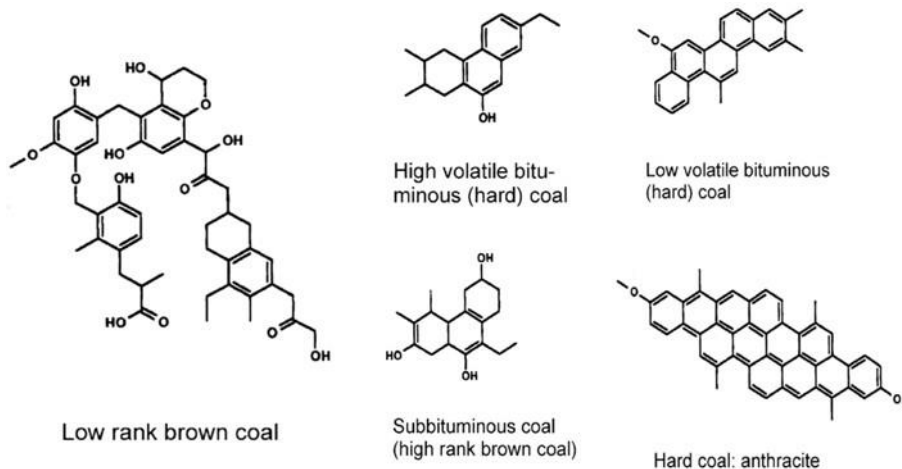
Figure 1. Different types of coal [30]

Lignite application for remediation purposes has received global attention due to the attractiveness of this material for pollution remediation because of its readily availability, cost-effectiveness, and possession of suitable characteristics responsible for effective adsorption of contaminants from aqueous media [31]. Through adsorption, oxygen functional groups in brown coal can bind Cr(VI) and Cr(III), while simultaneous reduction of Cr(VI) to Cr(III) by OM and Fe(II) may occur for easy Cr removal [32]. This has indicated that brown coal-based adsorbents are excellent sorbent suitable for efficient treatment of Cr-contaminated wastewater bodies and soil systems [33]. Hexavalent chromium and Cr(III) redox transformations are strongly influenced by soil properties and microorganisms.

Humic substances found naturally in the environment have the capability to adsorb Cr(VI) over a wide range of pH values and subsequent reduction to Cr(III) [34]. The main components in metal sorption are the predominating large amounts of humic (HA) and fulvic acids [35]. Humic acids can enhance removal of Cr(VI) through Cr(III) complexation as surface-bound HA, and Cr(III)-HA complexes adsorption phenomena or reduction of Cr(VI) by Fe(II) under sub-oxic conditions [36, 37]. Humic acids possess various properties including density of phenolic and hydroxyl sites in the humic substances and the reactivity of the HAs are directly related to both the reduced chromium, Cr(III) / reduction of Cr(VI) mobility and the total capacity of reduction [38, 39]. Organic matter in the environment often contain HAs, which intend possess high phenolic, hydroxyl and aldehyde moieties capable of reducing Cr(VI) to

12

Cr(III) [40]. Moreover, younger sources of OM such as sewage sludge, compost are preferred in metal remediation because of their possession of more labile humic substances [34].

3.2.3 Remediation of arsenic and chromium contaminated soils by phytoextraction

Phytoremediation is a promising, environmental-friendly and less expensive technology that utilizes plants to extract, degrade and/or immobilize pollutants in water bodies and soil systems [41]. Plants utilized in phytomanagement should have the ability to make a balance between toxic oxygen derivatives production and possession of antioxidative defense systems serving as survival and tolerant mechanisms by plants under stress conditions [42].

The concept of phytoremediation was first studied by Chaney in the 1980s, which later adopted the use of plant species for environmental soil contaminants remediation [43]. This term simply means applying hyperaccumulator plants genetically engineered for environmental clean-up of contaminants [44]. Phytoremediation presents various advantages such as environmental-friendliness, cost effectiveness, utilization of plants for extraction and degradation of pollutants in water bodies and soil systems [45]. Several plants have been employed in HM remediation which include Moso bamboo alongside *S. plumbizincicola,* cattail (*Typha latifolia*) and vetiver (*Chrysopogon zizanioides*), *Pteris vittata* and cash crop *M. alba*, sorghum (*Sorghum bicolor L.*) and oat (*Avenasativa L.*), eucalyptus (*Eucalyptus tereticornis Sm.*), subabul [*Leucaena leucocephala* (*Lam.) de Wit*], dhrek (*Melia azedarach L.*) and shisham (*Dalbergia sissoo Roxb.*) [46], Parthenium, Cannabis, Euphorbia, Rumex species, *Arabidopsis thaliana*, *Cannabis sativa*, *Albizzia lebbek,* duckweed (*Lemna minor*) [47, 48], Panikum *(Panicum antidotal),* Napier grass *(Pennisetum purpureum),* squash *(Cucurbita pepo),* cotton *(Gossypium hirsutum),* sunflower *(Helianthus annuus),* alfalfa (*Medicago sativa), Vinca rosea, Vigna mungo* plants [49]. Plant growth promoting bacteria (PGPB) also have the potential to minimize metal toxicity and enhance growth of plants in HM-stressed soil conditions [11].

During biotransformation of HMs and metalloids by plants through phytoremediation, plants utilize defense mechanisms such as oxido-reductive enzymes like laccase, oxidases, lignin peroxidase, tyrosinase, azo reductase, DCIP reductase, superoxide dismutase (SOD), catalase (CAT), peroxidase (POX), ascorbate peroxidase (APX), glutathione reductase (GR) and low-molecular weight quenchers like ascorbic acid, thiols and proline [50]. Phytochelatins (PCs) and

metallothioneins (MTs) cysteine-rich protein molecules also have the ability to bond and immobilize Cr(VI). Some of these antioxidative enzymes are responsible for detoxification of free radicals resulting from metal ions thereby remediating soils contaminated by metals and metalloids [48, 49].

3.2.4 Application of biochar for heavy metal/metalloid stabilization in soils

Application of biochar (BC) for soil amendments have gained considerable interest because of their potential in decreasing metals/metalloids mobility and bioavailability in contaminated soil systems [51]. Biochar is an environment-friendly porous carbon-rich material produced under low oxygen conditions, which possesses huge specific surface area, stable structural capacity with greater absorption capabilities. Biochar could be produced from readily available waste materials [52, 53]. The micro- to mesoporus structures, different surface functional groups including carboxylic, hydroxyl, carbonyl, alcoholic, and lactone groups and some inorganic mineral species (e.g., $CaCO_3$, PO_4^{3-}) are responsible for BC ability to adsorb contaminants from soil environment [54, 55]. Nevertheless, BC presents several advantages such as nontoxicity, richness in OM for the improvement of crop yield, excellent porous structure, possession of high CEC, soil pH enhancement, greenhouse gas emission reduction as well as easy dispersion, which is responsible for stabilization and reduction of contaminants mobility in soil [56, 57]. Oftentimes, BC is utilized because of certain characteristics encompassing biochemical stability, decomposition resistance, long-term soil organic carbon storage, increased nutrient availability, enhanced soil water storage capabilities and decreased toxic effects of HMs through adsorption from soil thereby reducing their uptake by plants [58, 59]. However, one important setback associated with soil amendment using charcoals (a type of BC) is that, their homonuclear constitution adsorb contaminants mainly through van der Waals interactions [60, 61]. Additionally, sorption of As oxyanions onto BC surfaces could be restricted due to the predominance of negatively charged surface of BC. Therefore, engineered BCs have been developed to enhance sorption capabilities of BCs by modifying their physical and chemical properties for organic and inorganic contaminants stabilization [62, 63]. Application of activated BC can be useful in stabilizing metals/metalloids in soil systems. To improve the efficacy of

stabilizing materials for soil amendment, two or more stabilizing agents should be combined to improve and mutually complement their properties [64].

3.2.5 Compost and organic material usage for heavy metal/metalloid stabilization in soils

Organic matter is important biomaterial which could be utilized for HMs/metalloids mobility reduction through adsorption, complexation and redox reactions [65, 66]. Application of organic amendment to contaminated soils could effectively reduce the bioavailability of HMs/metalloids by transforming them into organic-bound form, thereby reducing the water soluble and exchangeable fractions in the soil system [67, 68]. The advantages of amending contaminated soil are that, it plays the role of organic fertilizer by promoting crop development and improves the physical and chemical properties of the soil [69]. Additionally, application of other amendments such as $Fe(NO_3)_3$ with peat inhibits Fe(III) reduction and/or stimulates nitrate-dependent Fe(II) oxidation resulting in Fe-As coprecipitation or As adsorption onto Fe(III) minerals in soil. Functional groups in peat and As are known to form a bridge with Fe and subsequent formation of ternary complexes leading to As immobilization [65]. It is recommended to combine OM treatments with other stabilizing materials like Fe oxides, $Fe(NO_3)_3$ or slurries to achieve effective bioremediation of trace element contaminated soils through simultaneous adsorption and coprecipitation of contaminants by individual stabilizing agents [66, 67].

Compost as the stabilized form of OM contains high quality nutrients, which can be applied to agricultural soils as organic fertilizer and can effectively reduce metal/metalloid mobility in contaminated soil system [68, 69]. Not only does compost serve as fertilizer and replenish various soil nutrients, it also improves soil physicochemical properties by increasing microbial biomass [70, 71]. Numerous farm residues like manures and slurries as well as urban residues among others could also be utilized for compost production and applied for trace element contaminated soils bioremediation [72, 73].

Overtime, soil-retained HMs/metalloids could be solubilized under environmentally favorable and OM decomposing conditions [74]. Therefore, it is imperative to combine compost amendments of varied ratios with other stabilizing materials to help increase pH, resist

dissolution and, eventually prevent the release of stabilized metals/metalloids back into the soil system [75].

3.2.6 Soil washing and electrochemical remediation for arsenic and chromium contaminant removal

Electrokinetic remediation (EKR) is an effective, environmentally friendly, *in situ* remediation technique employing direct or alternating current for the decontamination of many pollutants. These contaminants include HM contamination, sewage sludge, organic pollutants, wastewater and dredged sediments. Several advantages are associated with EKR including; environment-friendliness, compatibility, multifunctionality, adaptability and lower conditions of reactivity [76-78]. The two mechanisms, electromigration and electroosmosis coupled with acidification to generate H^+ govern metals or metalloids transportation by solubilizing/mobilizing elements in the anode causing precipitation at the cathode due to high concentration of OH^- [79]. Water moves to the cathode leading to immobilization of metal/metalloid contaminants or metals/metalloids associated with oxide, hydroxide and carbonate immobilization [80, 81]. Not only is this technique useful for contaminant immobilization, EKR could be employed to simultaneously recover metals/metalloids and remediate contaminated soils, as well [82]. Oxidation of Mn(II) through electrochemical catalytic oxidation inducing conversion of As(III) to As(V) is an alternative to reduce As contamination in soil system [83, 84]. When the approaching anodes electrokinetic (AAs-EK) technique is applied to suitable reducing agents like sodium bisulfite ($NaHSO_3$), there is increase in the HM concentration attributable to possible dissolution of Fe- and Mn-bound minerals in the soil system [85].

Soil washing simultaneously recovers and recycles HMs and permanently remediate contaminated soils [86]. Biodegradable agents are useful in soil washing and possess strong complexing capacity, high biodegradability and lower toxicity to microorganisms and plants. These agents could be employed for chelating to mobilize soil contaminants by forming soluble complexes to prevent long-term liability and subsequent phytoextraction by plants [87, 88]. Certain soil extraction agents are unable to efficiently remediate contaminated soils due to hindrances associated with their easy precipitation and rapid decomposition properties [89, 90]. The use of synthetic chelating agents [e.g. (S,S)-N,N′-ethylenediamine disuccinic acid (EDDS)]

promote amorphous Fe/Mn oxides dissolution to enhance metal/metaloid extraction [91, 92]. However, application of multiple chemical agents like reductants, alkaline solvents, and organic ligands to metals/metaloids and strongly bound to Fe/Mn oxide - metalloids contaminated soils is necessary to achieve effective immobilization rates [93-95]. Alkaline solvents with higher alkalinity are superior in removing As from contaminated soils due to their higher hydroxyl-promoted dissolution of As-associated mineral oxides. And also, the subsequent inhibition of As re-adsorption as a result of electrostatic repulsion after dissolution make these alkaline solvents preferred choice [96, 97]. Other effective soil cleaning procedures employ suitable chelating agents such as ethylenediaminetetraacetic acid (EDTA) coupled with microwave radiation heating system or citric acid/sodium citrate (CA/SC) washing process [98, 99].

3.2.7 Stabilization of arsenic and chromium in soils by oxides and/or hydroxides, natural and modified iron-containing minerals

Iron minerals are important immobilizing agents and through formation of amorphous Fe oxides metals/metalloids are exposed to more active adsorption sites [100-102]. Other phenomena affecting metal/metalloid availability in soil systems are alternating cycles including wetting and drying of the soil which could cause changes in pH, redox potential, ionic strength, hydrolysis of Fe^{2+} and Fe^{3+} in oxidizing environment. The resulting Fe solid formation, Fe-OM coprecipitation and oxygen secreted by plant roots may affect bioavailability of metals/metalloids [74, 103].

Generally, *in situ* immobilization of As associated to Fe oxides, Fe hydroxides, and iron Fe containing materials, result in significant reduction in As bioavailability in soil, thereby decreasing As translocation, accumulation in crops and transfer into the food chain [104, 105]. Trivalent arsenic oxidation on Fe oxide surfaces may occur in the presence of light, Fe oxides, Fe hydroxides or Fe containing materials [106, 107]. Moreover, metals/metalloids contaminants sequestration by iron oxy-hydroxides (α-FeOOH) (goethite), surface complexation between hydroxyl groups of Fe(II)-modified zeolite, modified alumina-silicates could lead to the contaminants stabilization in soil systems [108, 109].

Development of a novel techniques such as nanoremediation which includes nanoscale zero valent iron nanoparticles (nZVI-NPs) for HMs/metalloid immobilization have proven useful in *in situ* stabilization of As in soils [110, 111]. It has been demonstrated that nanozerovalent BC

(nZVI-BC) can improve the stability and reduce metal/metalloid mobility and, hence minimize upward translocation of metals/metalloids into plants from soil system [112]. Numerous sorption sites of nZVI-BC are responsible for the higher colloid stability and strong reduction reactivity for Cr(VI) remediation [113, 114]. However, optimum application rates of nZVI to BC is important to ensure efficient particle dispersion in order to avoid nZVI particles aggregation and enhance Cr(VI) removal [115]. Usually, nZVI possess higher reactivity due to their acicular shapes, which intend to increase the specific surface of granular Fe [116]. These nanomaterials like crystal particles loaded with bismuth oxide or bismuth oxychloride have the potential to improve the specific surface area of BC by creating additional micropores [117, 118]. Similarly, enhancement of active sites and amorphous iron/aluminum oxides of sludge-derived BC (SDBC) can influence immobilization of anionic metals [119, 120].

3.2.8 Role of functional groups, pH, CEC on metal and metalloid stabilization in soils

Soil sorption capacity is highly dependent on pH of the soil system, whereas CEC is responsible for adsorption route by increasing sorption sites, promoting higher binding affinity and reducing metal mobility [121-123]. It is based on these characteristics that sand exhibits lower CEC due to lower binding power for metals as compared to clay soils, which show high binding affinity for HMs [124]. Biowastes materials like BC demonstrates higher binding capacities for metals because of their oxygen-containing functional groups (e.g. –COOH and –OH and –COO− and –O−) [125]. These functional groups are responsible for increasing the soil CEC, pH and pH-BC [126, 127]. Moreover, the soil pH increase is caused by organic anions emerging from the dissociation of abundant oxygen-containing functional groups contained in BC. These functional groups scavenge protons leading to metal/metalloid immobilization [127, 128]. In water systems, the presence of challenger co-ions viz. Cl^-, NO_3^-, HCO_3^- and SO_4^{2-} can slightly influence sorption capacity of hydroxocomplexes of Cr [129, 130]. Both monovalent (K^+ and Na^+) and divalent (Ca^{2+} and Mg^{2+}) cations can also influence the intensity and sorption capacity of hydroxocomplexes of Cr [131].

When BCs are impregnated with metals or metal oxides, the positively charged and activated adsorption site formation increase the specific surface area and number of functional groups. These sorption sites are responsible for removal of both positively charged ions and

18

negatively charged anionic contaminants through adsorption and electrostatic forces of attraction [132]. Additionally, stabilization of biowaste materials could be achieved through oxidation with strong oxidizing agents like concentrated oxyacid solutions to produce carboxylic, lactonic, phenolic, etc. functional groups [133, 134]. Higher plants roots are known to secret low-molecular-weight organic acids (LMWOAs) which could mobilize trace elements in rhizosphere. Based on this information, attempts have been made to treat BC with LMWOAs like OA to enhance the immobilization of oxyanions like iAs(V) through protonation [135, 136]. An alternative to improve and increase functional groups of biomaterials is to form composites from these materials [137].

4. Materials and Methods

4.1 Materials and reagents

Throughout the experiments, ultra-pure water of 18 MΩ cm resistivity was taken from an ELGA Purelab Option-R7 unit (ELGA LabWater/VWS Ltd., High Wycombe, UK) and used for sample preparations and dilutions. Concentrated (conc.) ammonia, conc. HNO_3, glacial acetic acid and conc. HCl were of Suprapur® (Merck, Darmstadt, Germany) quality. Hydroxylamine hydrochloride (Sigma Aldrich) was of analytical grade. For phytoavailability studies, analytical grade disodium salt of EDTA (Scharlau Srl., Barcelona, Spain) was used. The Cr(III) stock solution was prepared from analytical grade chromium(III) nitrate nonahydrate, purchased from Sigma–Aldrich (Budapest, Hungary).

Similarly, regarding the arsenic treatments, for carbonization, cc. sulfuric acid solution of analytical grade used was purchased from VWR International Ltd. (Debrecen, Hungary). The reagent grade 60–100 mesh Florisil® and Celite® S referred to as Celite® further on, were purchased from Sigma Aldrich (Budapest, Hungary). Florisil® is a white powder corresponding to synthetic magnesium metasilicate ($MgSiO_3$). Its structure consists of discrete units of $MgSiO_3$ activated at 675 °C. According to the manufacturer, it possesses a very large specific area (289 m^2/g) and is used as chromatographic adsorbent for polar molecules [138]. Celite® is a white powder corresponding to untreated diatomaceous earth consisting between 6 and 10% of amorphous SiO_2. Water molecules are contained in it in form of clathrates, the proportion of silanol groups (Si–OH) is low. These groups can be found not only on the surface but also in the bulk substance. Structurally, it resembles phyllosilicates, but it is not completely crystalline, there are several disturbed sites in it that also contain Si–OH groups. According to the manufacturer, the chemical composition of Celite® is the following: 4.1% Al_2O_3; 0.4% CaO; 1.6% Fe_2O_3; 0.2% MgO; 1.4% $Na_2O + K_2O$; 0.3% P_2O_5; 90.2% SiO_2 and 0.2% TiO_2. Among its properties, it should be emphasized a loss of 3.2–10.0% on ignition at 900° and pH≈7 (25 °C, 10% in aqueous suspension). It is normally used as filter aid material [139]. The iAs(V) stock solution was prepared from potassium dihydrogen arsenate purchased from Sigma Aldrich.

For calibration in the case of Cr determination, 1 g/L acidic Cr(III) and indium (In) (used as internal standard) stock solutions (Merck) were used after appropriate dilutions. For external

calibration and internal standardization for As, 1 g/L acidic iAs(V) and Ge stock solutions (Merck), respectively, were used after appropriate dilutions. The final HNO_3 concentration of each sample solution was set to 5% (v/v). Regarding the TXRF spectrometric analysis, the quartz carrier plates were hydrophobized in the same way with silicone in isopropanol purchased from SERVA Electrophoresis GmbH (Heidelberg, Germany) and the 1 g/L acidic yttrium (Y) ICP stock solution was also purchased from Merck.

Before sampling, the 50-mL centrifuge tubes were soaked in 20% (v/v) HNO_3 for several days and then rinsed with deionized water. All standard solutions were prepared daily from stock solutions via appropriate dilutions in polypropylene (PP) Falcon® centrifuge tubes (Fisher Scientific, Waltham, MA, USA).

4.2 Soil sampling and incubation

4.2.1 Soil sampling and incubation for studies involving lignite / iCr(III)

Samples used for these investigations were acidic and calcareous sandy soils taken from two Hungarian settlements, i.e. Nyírlugos (47°43′N, 22°00′E) and Őrbottyán (47°40′N, 19°14′E) and sieved to < 2 mm particle size fractions.

Lignite originating from the mines of Visonta, Hungary (Figure 2) was size-fractionated into three particle ranges (i.e. <0.5 mm, 0.5–1.0 mm and 1.0–2.0 mm) by sieving. Then, each fractioned sized was added to the soil samples at a dose of 5% by weight. The physicochemical parameters of the studied soils and lignite samples are listed in Table 1.
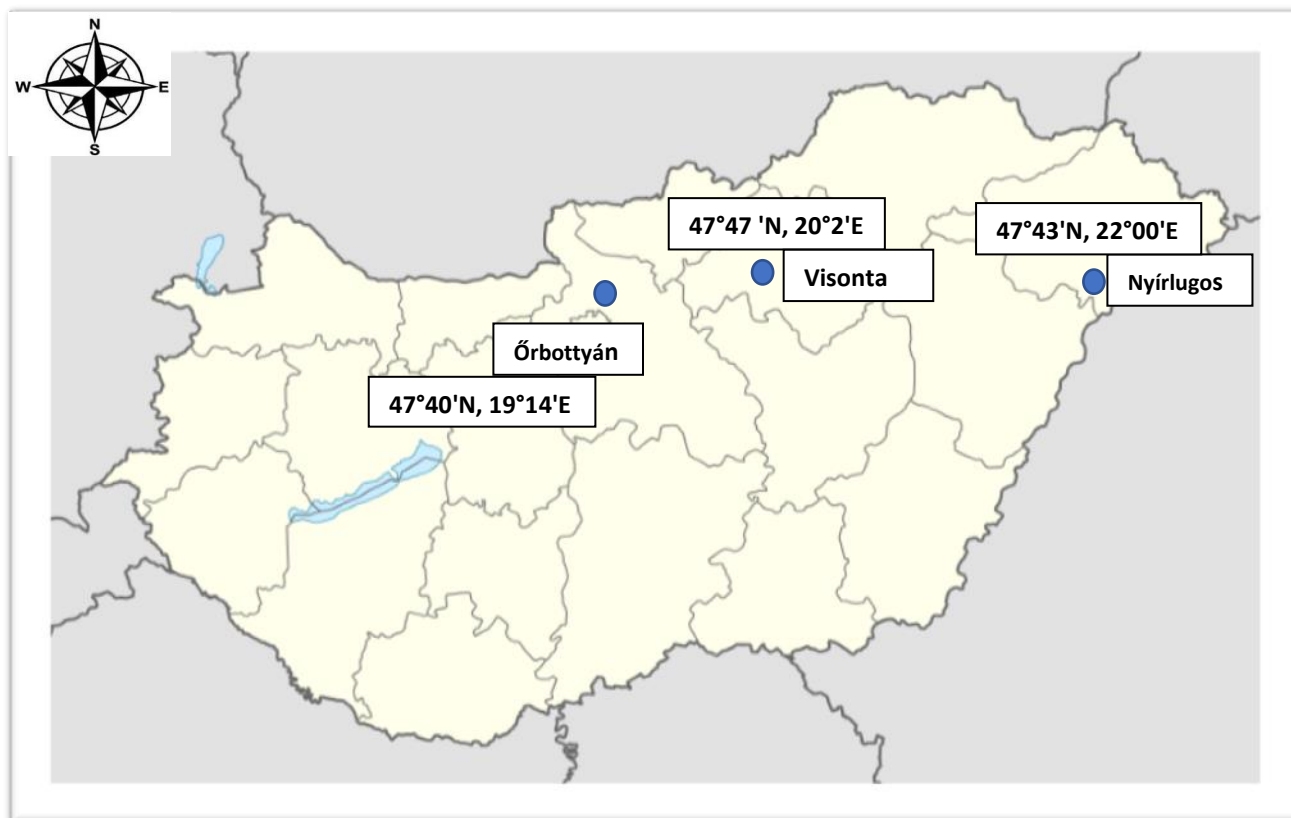
Figure 2. Map of Hungary showing sampling locations of soils and brown coal

Soils were artificially contaminated with 375 mg/kg of iCr(III). The acidic and calcareous air-dry soil samples were homogenized and amounts of each 1 kg were placed in non-perforated, polypropylene (PP) round pots (height: 22 cm; diameter: 12 cm). Appropriate aliquots of a iCr(III) stock solution prepared by dissolving $Cr(NO_3)_3 \times 9H_2O$ and lignite were added simultaneously to the soil and thoroughly mixed. Then, each PP pot was covered with tinfoil. Moreover, blank (n = 24) and control (n = 6) soil samples were each also prepared in triplicates. Control soil samples contained only iCr(III) in 375 mg/kg concentration. Blank samples contained either the soil itself or also lignite in the aforementioned different size fractions. For each type of treatment, three individual samples were considered. Thus, in total, 48 samples were prepared. Incubation of samples under controlled temperature (kept at 21°C) and moisture content (65% of field water capacity, monitored weekly) lasted for eight weeks. All experimental parameters were chosen based on a multi-factorial model design [140].

Table 1. Physicochemical characterization of the studied soil and lignite samples.

Parameter	Acidic sandy soil	Calcareous sandy soil	Lignite
pH	5.0	7.7	4.2
Upper limit of plasticity (K_A)	26	27	n.a.
Salt content (%)	<0.02	n.a.	n.a.
CEC (mEQ/100 g)	5	5	10
Sand, >0.05 mm (%)	85	81	n.a.
Silt, 0.05–0.002 mm (%)	10	13	n.a.
Clay, <0.002 mm) (%)	5	6	n.a.
Organic matter (%)	0.5	1.0	34.5
Specific surface area	Low	n.a.	n.a.
$CaCO_3$ content (%)	Traces	3.3	n.a.
Metal-binding capacity	Low	n.a.	n.a.
Aqua regia soluble Cr (mg/kg)	4	5	23.3
Aqua regia soluble Fe (mg/kg)	6,630	9,350	13,900
Aqua regia soluble Mn (mg/kg)	144	308	279

Abbreviations: CEC = cation-exchange capacity; n.a. = not available.

4.2.2 Soil sampling and incubation for studies involving activated charcoal / iAs(V)

The same acidic soil from Nyírlugos was sampled and sieved to grain size of < 2 mm (Table 1). The different granular AC varieties were prepared from roasted and unsalted peanut (*Arachis hypogea*) in shell originating from China and distributed in Hungary by Mogyi Ltd. (Csávoly, Hungary). A primary sample of about 10.5 kg peanuts in shell consisting of seven increments (six packages of about 1.5 kg each and one of about 1 kg) taken from a bulk sample sold in a hypermarket in Budapest (Hungary) was further used. The composite sample obtained by combining the individual portions was shelled manually in the laboratory. After separation from the kernel, shells were ground and sieved to 1 × 1 mm particle size in a mortar grinder (Retsch

GmbH, Haan, Germany). The resulting ground shell weighed about 3.5 kg. For the charcoal preparation, ground shell subsamples of about 100 g were used. Carbonization of a subsample was achieved in a crystallizing dish in a fume cupboard with 140 mL of cc. H_2SO_4 added in aliquots of 1–2 mL under continuous stirring with a glass rod. Further enhancement of functionalization was attempted after 5–10 min with 25 mL of cc. HNO_3 solution also added in aliquots of 1–2 mL under continuous stirring [141].

Another shell subsample of 100 g was mixed with either 30 g each of Celite® [142] or Florisil® prior to addition of cc. H_2SO_4 solution. Charred samples were kept in an oven at 150 °C for one additional day. After this step, the resultant charcoal samples were soaked in 1 L of UPW every 3 h until the specific electric conductivity of the decantated liquid phase, determined by an FE30/FG3 conductivity meter (Mettler Toledo Ltd., Budapest, Hungary), decreased to 30 µS/cm. At the same time, pH of the leachates determined by an OP-211/2 pH meter (Radelkis, Budapest, Hungary) was about 3.5. The ACs were dried in an oven at 105 °C for one additional day, then sieved (1 mm mesh size). Sample mass loss compared to the initial ground and sieved shell was about 50% for functionalization with cc. HNO_3, while this reduction for experiments conducted with Celite® and Florisil® was equally about 40%.

Sample treatments with the corresponding codes are summarized in Table 2. These codes will be used further on in the text, while all the procedures are illustrated in Figure 3.
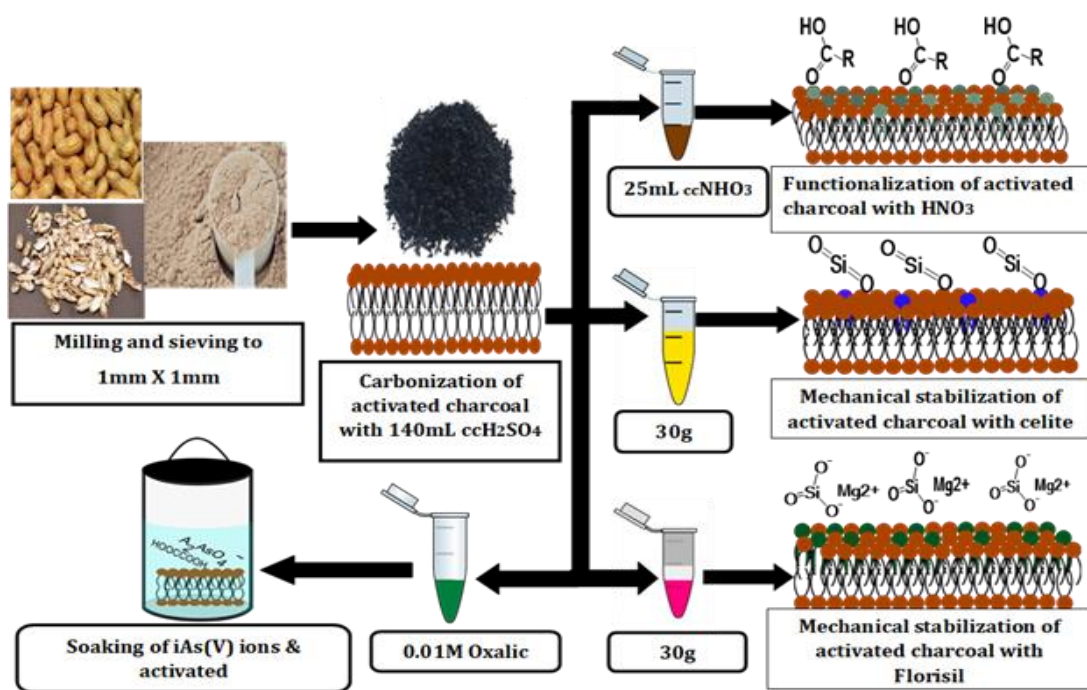
Figure 3. Procedure adopted in the activated charcoal preparation

Table 2. Sample treatments involving iAs(V) and diffente types of activated charcoal

Sandy soil	iAs(V) (mg/kg)	AC type	AC (m/m%)	Treatment code
acidic	-	-	-	SAs_0AC_0
acidic	15	-	-	$SAs_{15}AC_0$
acidic	30	-	-	$SAs_{30}AC_0$
acidic	15	reference	2	$SAs_{15}RAC_2$
acidic	30	reference	2	$SAS_{30}RAC_2$
acidic	15	reference	5	$SAs_{15}RAC_5$
acidic	30	reference	5	$SAs_{30}RAC_5$
acidic	15	HNO_3	2	$SAs_{15}Nitric\text{-}AC_2$
acidic	15	Celite®	2	$SAs_{15}Celite\text{-}AC_2$
acidic	15	Florisil®	2	$SAs_{15}Florisil\text{-}AC_2$
acidic	30	Florisil®	2	$SAs_{30}Florisil\text{-}AC_2$
acidic	15	Florisil®	5	$SAs_{15}Florisil\text{-}AC_5$
acidic	30	Florisil®	5	$SAs_{30}Florisil\text{-}AC_5$
acidic + 0.1 M oxalic acid	-	Florisil®	2	$SOAAs_0Florisil\text{-}AC_2$
acidic + 0.1 M oxalic acid	15	Florisil®	2	$SOAAs_{15}Florisil\text{-}AC_2$

For the As soil samples treatments (Table 2), portions of 250 g soil was used. Generally, the prepared AC was added in a mass fraction of 2.0 wt% to the soil samples. In most of the cases, soils were homogenized with 15 mg/kg As in form of iAs(V). In the case of the reference AC (i.e., ground peanut shell charred with cc. H_2SO_4 solution) and that modified by Florisil®, an AC application rate of 5 wt% as well as 30 mg/kg iAs(V) treatment have also been applied (Table 2). In another experiment, 250 g of the same soil was mixed with 2 wt% Florisil® containing AC. Then, 100 mL of 0.01 M OA solution was added to this soil system. The resulting suspension was homogenized in a rotary shaker for 1 h. After filtration, pH of filtrates were measured. Then, the treated soil samples were dried in an oven at 105 °C prior to further treatment with iAs(V) (Figure 3).

Incubation of samples ($n = 3$) placed in PP pots under controlled temperature (21 °C) and moisture content (65% of field water capacity) lasted for 1 month. The moisture content of the samples was adjusted weekly were it was necessary. Control soil samples either containing iAs(V) or not were also prepared and incubated the same as described above. All experiments were performed in triplicate. The treatments have been illustrated (Table 2).

4.3 Soil extraction procedures

4.3.1 Modified BCR leaching soil extraction procedure

In the elemental mobility investigations, a modified Community Bureau of Reference (BCR) European Commission, soil leaching procedure [143] consisting of two steps was applied as summarized in Figure 4. Briefly, the extraction of the water soluble and carbonate bound fraction were leached together with 0.11 mol/L acetic acid solution. This step was followed by extraction of the fraction bound to amorphous oxides of Fe(III)/Mn(IV) by the use of 0.5 mol/L hydroxylamine-hydrochloride solution of pH=2. The step used for leaching oxidizable species was obviously omitted as the trace element uptake by the plants is more likely to be achieved through reduction process. In the leaching procedure, the sample mass and extractant volume ratio was set to a ratio of 1 to 40 in both leaching agents. Samples were shaken for 16 h at 30 rpm by an endover-end shaker (IKA® Works Inc., Staufen, Germany). After the extraction, the

26

samples were seperated by centrifugation at 4500 rpm for 15 min performed in a tabletop centrifuge (Hermle Labortechnik GmbH, Wehingen, Germany) and supernatants were decanted into PTFE digestion vessels. Finally, microwave (MW)-assisted digestion of the leachate residues with *aqua regia* was applied to obtain the *pseudo*total fraction.
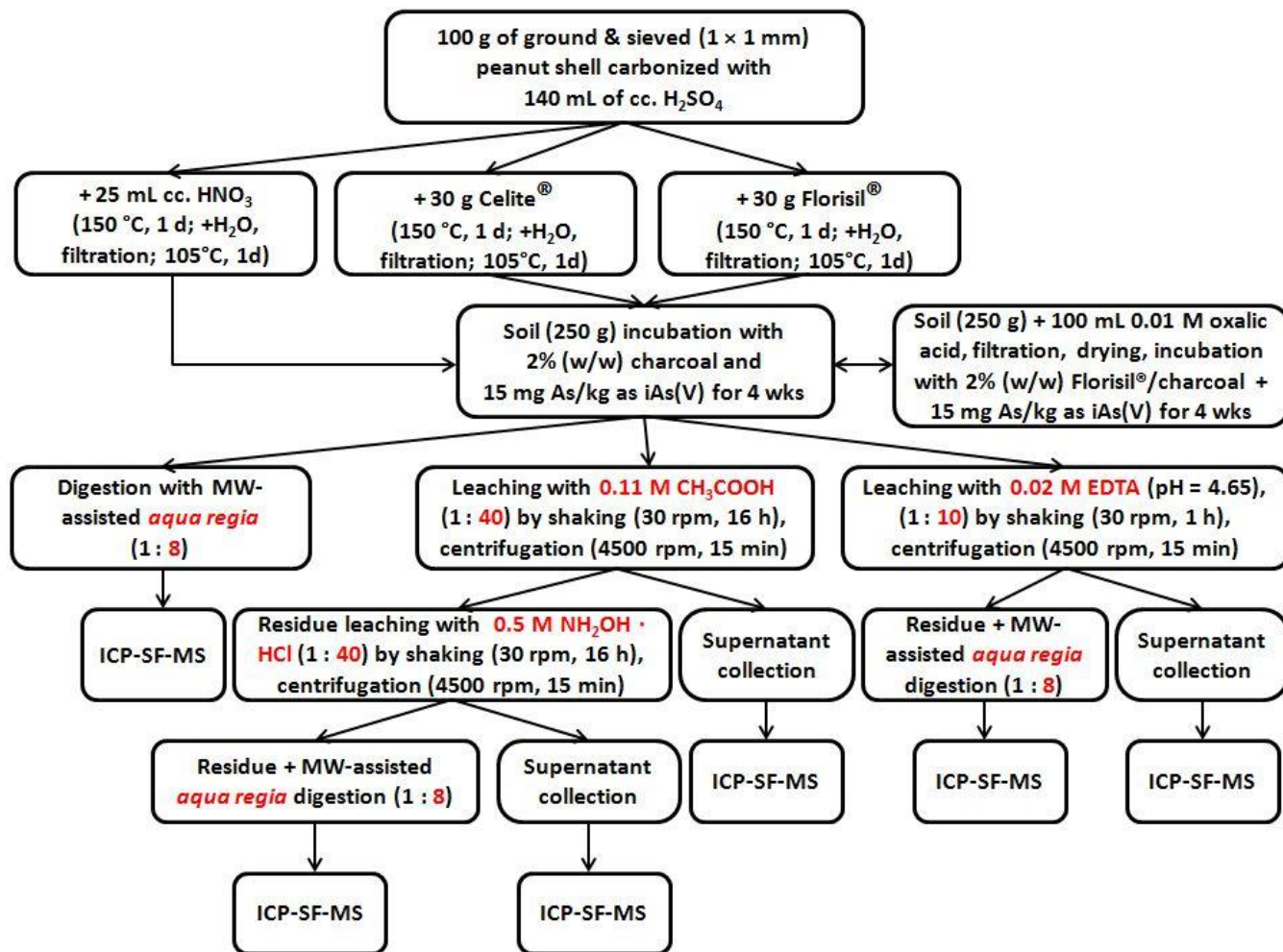
Figure 4. Schematic diagram of the sample preparation steps and analysis performed on the investigated soil samples. BCR = Community Bureau of Reference, European Commission

4.3.2 Phytoavailability experiments

The phytoavailable fraction of the samples was determined according to the Lakanen – Erviö soil leaching procedure [144]. Briefly, soil samples were extracted for 1 h with 0.02 mol/L EDTA solution of pH≈4.65 (Figure 4). This pH value was set with conc. NH_3 by using an OP-212/2 pH-meter (Radelkis Ltd., Budapest, Hungary). The soil mass and extractant volume ratio was set to a

ratio of 1 to10. After the extraction was completed, centrifugation was applied as described in Figure 4. Finally, the same MW-assisted digestion method with *aqua regia* was applied for the leachate residues.

4.4 Inductively coupled plasma mass spectrometric methods

Prior to elemental analysis, the initial samples, as well as the leachate residues were subjected to MW-assisted *aqua regia* digestion performed by an Ethos Plus 1 equipment (Milestone S.r.l., Sorisole, Italy) according to the slightly modified EU Standard EN 13346 (2000) [145]. Briefly, each 1.0 g of the homogenized samples was transferred into 100-mL PTFE digestion vessels (n = 5). Then, 8 mL of *aqua regia* was added to the samples. The steps of the MW-assisted digestion program were as follows: 500 W for 4 min; 750 W for another 5 min and finally, 800 W for another 12 min. The upper temperature limit was 170°C. After the digestion was completed, the vessels were cooled and the digested samples were decanted into PP tubes and diluted (1000-fold) for HNO_3 concentration to be set as 5% (v/v). Concentrations of Cr, Mn and Fe were determined by inductively coupled plasma sector field mass spectrometry (ICP-SF-MS) performed on an Element 2 equipment (Thermo-Fisher Scientific, Bremen, Germany). The acetic acid, hydroxylamine and EDTA leachates were analyzed directly after proper dilutions.

For these determinations, 50 µg/L In was used as internal standard. The internal standard for the As determination was Ge in 20 µg/L concentration. The optimized operating conditions for the ICP-SF-MS measurements were as follows: RF power = 1200 W; carrier, auxiliary and nebulizer Ar flow rate: 14, 1.0 and 1.0 L/min, respectively. Meinhard nebulizer equipped with a Scott spray chamber was used for nebulization of the samples. The diameter of the sampler and skimmer cones both made of Ni were of 1.0 and 0.8 mm, respectively. For monitoring of the $^{75}As^+$ counts by the electron multiplier and separation of those corresponding to $^{40}Ar^{35}Cl^+$, the ICP-SF-MS instrument was operated in the high resolution (R = 10,000) mode. Peak jumping was used as scan mode. Dwell time was 0.1 s. In the case of Ge, counts of the ^{74}Ge isotope were monitored.

The optimized operating conditions for the ICP-SF-MS measurements and the monitored isotopes are listed in Table 3.

Table 3. Optimized operating conditions of the ICP-SF-MS measurements and monitored isotopes

RF power (W)	1200
Carrier gas (Ar) flow rate (mL/min)	14
Auxiliary gas (Ar) flow rate (mL/min)	1.0
Nebulizer gas (Ar) flow rate (mL/min)	1.0
Nebulizer	Meinhard (equipped with Scott spray chamber)
Ni sampler cone diameter (mm)	1.0
Ni skimmer cone diameter (mm)	0.8
Resolution (R)	10000 (high)
Scan mode	Peak jumping
Dwell time (s)	0.1
Detector	Electron multiplier
Monitored isotopes	^{52}Cr, ^{55}Mn, ^{56}Fe, ^{74}Ge, ^{75}As, ^{115}In
Internal standard	50 µg/L In for Cr, Fe & Mn
	20 µg/L Ge for As

Abbreviation: ICP-SF-MS – inductively coupled plasma sector field mass spectrometry.

4.5 Total-reflection X-ray fluorescence analysis for quality assurance

The TXRF measurements were carried out on an ATOMIKA Model TXRF 8030C spectrometer (ATOMIKA Instruments GmbH, Oberschleißheim, Germany), equipped with a Mo-W mixed anode X-ray tube operating at 50 kV and 47 mA. For excitation, the K_α line of Mo was used. The energy calibration of the instrument was performed prior to analysis, and periodically during the measurements with 100 ng of Ni was applied as reference standard. Attenuation of the background intensity was achieved by using a double layer ZrO_2 filter. Detection of fluorescent photons was performed with an energy dispersive Si(Li) semiconductor detector fitted with an 80 mm^2 entrance window, continuously cooled with liquid nitrogen. Signal processing was done by

a recording unit consisting of a (pre)amplifier, an analogue-digital converter and a multichannel analyzer.

For hydrophobization to determine Cr concentration, 10 µL of silicone solution in isopropyl alcohol was dropped onto the surface of the quartz carriers and were then dried at 110°C on a hot plate. An amount of 2.5 µL of the sample, containing 100 µg/L Y as internal standard, was dropped onto the hydrophobized carriers. After drying the samples at 80°C, the dried samples were placed into the TXRF equipment. The signal acquisition time was 100 s and 1000 s for energy calibration and analysis, respectively. For the analysis, the signal of Cr K_α line at 5.415 eV was recorded.

With the arsenic concentration determination by TXRF, 5 µL of the samples containing 100 µg/ L Y as internal standard was dropped onto the hydrophobized carriers. After drying of the samples at 80 °C, the quartz carriers were placed into the TXRF equipment. The signal acquisition live time was 100 s and 1000s for the energy calibration and analyses, respectively. For TXRF analysis, the acetic acid, hydroxylamine, EDTA leachates as well as the extraction residues and initial soil samples subjected to MW-assisted *aqua regia* digestion were diluted 5, 2, 25, 25 and 25 times, respectively.

4.6 Determination of lignite porosity

Nitrogen physisorption measurements were performed at -196°C using an automated volumetric adsorption analyzer (Thermo Scientific Surfer gas adsorption porosimeter, Bremen, Germany). Before use, lignite samples were degassed under high vacuum ($<10^{-6}$ mbar) at 200°C for 2 h. The specific surface area was calculated by the BET equation at 0.01–0.2 relative pressure. Before each test, the coal sample of 1–2 g in weight was degassed for 12 h at 383 K to remove air, water and other volatile matters. At each pressure set point, the sorption equilibrium was established automatically when the pressure stabilized for 30 s. The absolute pressure tolerance was set as 5 mmHg (6.66 mbar). Pore size distribution was evaluated from the adsorption branch, according to the BJH method. Micropore volume was calculated by the α_s plot method. The mesopore volume was calculated as the difference of the total pore and micropore volumes.

Scanning electron microscopy (SEM) studies were performed on a model Quanta 3D apparatus (FEI, USA) equipped with a secondary Everhart-Thornley detector and back-scattered

electron detector together with silicon drift energy-dispersive detector. For the measurements, 20 kV accelerating voltage, 15–480 pA probe current and 50 s as lifetime were used.

4.7 Determinationn of point of zero charge for lignite

The point of zero charge (PZC) of the different lignite samples was determined in 25 mL of 0.001, 0.01 and 0.1 mol/L NaCl solutions by applying the pH drift method [146]. Briefly, the pH of the samples was adjusted between 1 and 12 (n = 10) using proper amounts of NaOH or HCl solutions and the initial pH of the solutions was recorded. Then, lignite was added to these solutions in an identical application rate to that one used for the soil incubation (i.e. 5% by weight). After 24 h of shaking at 30 rpm by using the IKA$^®$ end-over-end shaker, the suspensions were filtered through Whatman microfiber glass filters (diameter: 2 mm) by using a 12-port Visiprep$^®$ solid-phase extraction vacuum manifold (Sigma-Aldrich). The PZC values were determined by plotting the ΔpH (final pH – initial pH) vs. initial pH. The point of intersection of the resulting curve with the abscissa (i.e., at ΔpH = 0), gave the PZC values.

4.8 Adsorption of arsenate onto activated charcoal from solutions

About 0.05 g AC (charred with sulfuric acid was used as reference), HNO$_3$- and Florisil$^®$-modified composites, respectively, were loaded with 25 mL of solutions containing 50–800 mg/L iAs(V) ($n = 3$). Then, the pH was set to 5 [and to 8 in the case of the Florisil$^®$-modified AC loaded with iAs(V)]. After 1 h shaking (Orbital Shaker OS-20, Biotech, Prague) at 400 rpm, the As-loaded AC was filtered through 0.8 μm pore size quartz fiber filters by the use of Visiprep SPE vacuum manifold (Sigma Aldrich) and dried at room temperature. The As concentrations of supernatants were determined by ICP-MS *cf.* (Table 3). These values corresponded to the equilibrium concentrations in the liquid phase (c_e), while the equilibrium concentration in the solid phase (q_e) was expressed as the mass of adsorbed As (mg) divided by the AC mass (g). Then, the ln c_e and ln q_e pairs were plotted for studying whether adsorption could be fitted by the Freundlich isotherm model (Eq. 1). This adsorption isotherm is mathematically expressed as:

$$q_e = K_F \times C_e^{1/n} \tag{1}$$

where; K_F = Freundlich constant and n = exponent indicating the degree of non-linearity. This exponent is calculated as the reverse of the slope of the linear fitting of the q_e vs. C_e plots. The Langmuir adsorption model (Eq. 2), expressed as:

$$q_e = \frac{q_{m,L} \ K_L \ C_e}{1 + \ K_L \ C_e} \qquad (2)$$

Where; $q_{m,L}$ = maximal adsorption capacity and K_L = Langmuir constant, has also been considered. Thus, linear fitting was also performed on the plotted c_e/q_e vs. c_e data pairs to check validity of this model of the investigations.

4.9 FT-IR analysis of the prepared activated charcoal

Fourier-transform infrared (FT-IR) spectra were recorded on the prepared AC in the attenuated total reflection (ATR) mode by means of a Varian 2000 instrument (Scimitar Series). The FT-IR spectrometer was fitted with a mercury cadmium telluride detector and a single reflection diamond ATR accessory (Golden Gate). A 4 cm^{-1} spectral resolution and 64 scans were applied. Baseline correction was made by GRAMS/AI software. Moreover, ATR-FT-IR analysis was also performed on Florisil®-modified AC loaded with 400 mg/L iAs(V). For this experiment, 2 g of charcoal was stirred in 200 mL of 400 mg/L iAs(V).

5. Results and Discussion

5.1 Optimization of lignite particle size for mobility reduction of trivalent chromium in soils

5.1.1 Porosity and point of zero charge characteristics of lignite samples

Porosity of the different lignite fractions used in the present study has been proven by means of SEM measurements (Figure 5). Porosity of lignite can be expressed by the pore volume, pore size distribution, mean pore diameter and micropore or mesopore surface area [147]. Pore accessibility of microporous materials is limited, while macroporous materials show low selectivity for different contaminants. That is why mesoporous materials can represent a compromise.
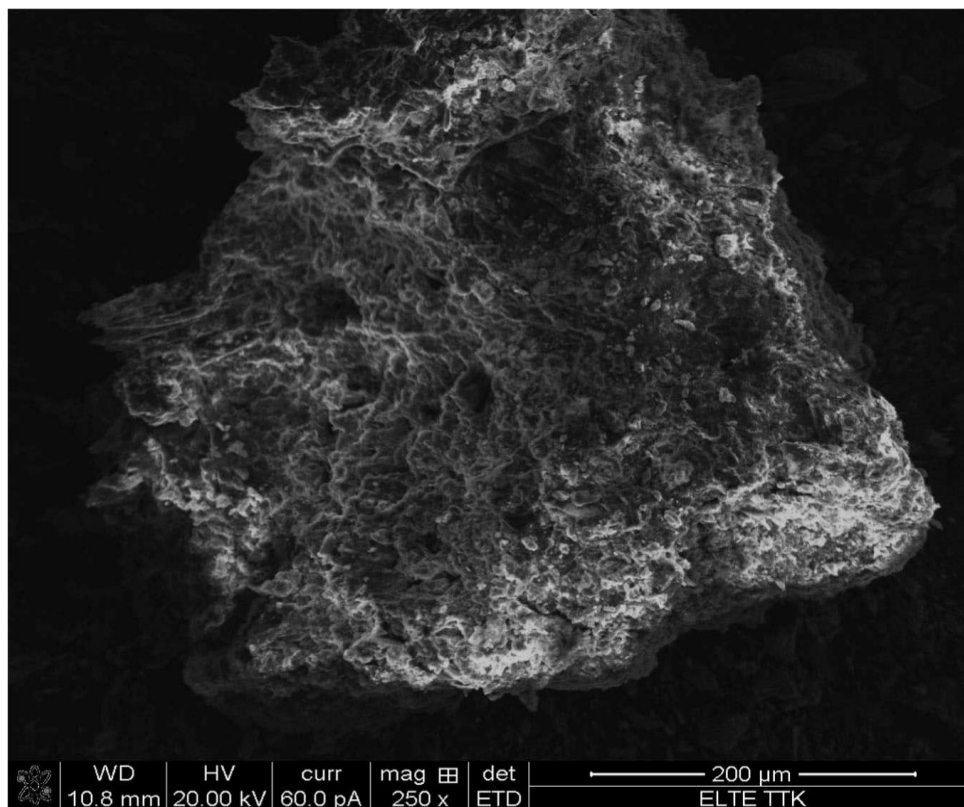

Figure 5. Scanning electron microscopic image of a representative lignite particle in the 0.5–1.0 mm at 250-fold magnification, registered at 20 kV and 60 pA

The mesoporosity characterization of raw lignite by studying N_2 adsorption–desorption is a common procedure. The adsorbed volume of nitrogen by raw lignite was observed to be low (Figure 6), which is in agreement with literature data [147]. All isotherms showed an H3 hysteresis loop. The specific surface area of raw lignite calculated by the BET method did not exceed 5 cm^2/g. The total pore volume was below <0.021 cm^3/g. However, this volume increased by 2.2 and 3.7 times when the lignite particle size from 1.0 to 2.0 mm and 0.5–1.0 mm was decreased down to <0.5 mm, respectively (Table 4).
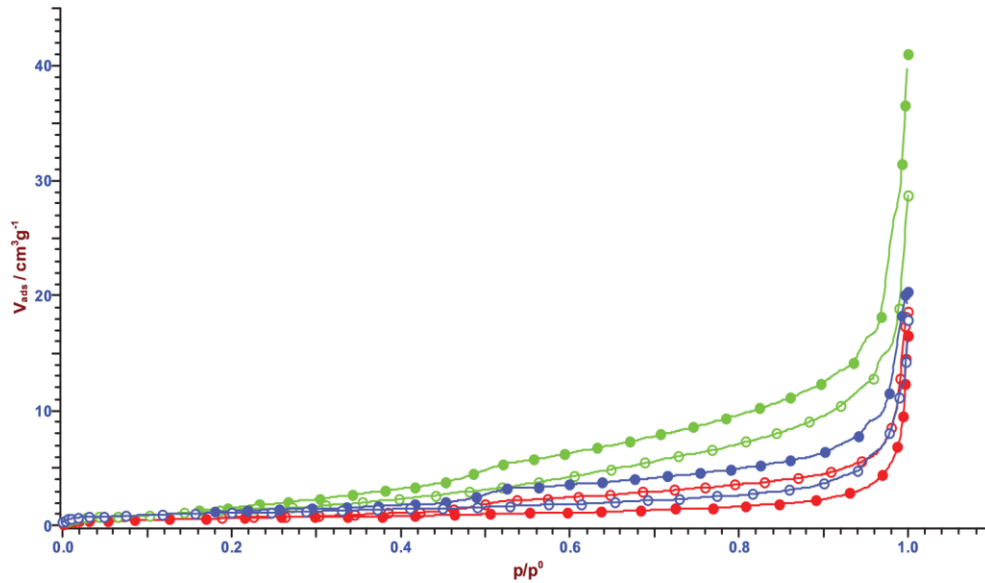
Figure 6. Nitrogen gas adsorption-desorption isotherms of the studied lignite samples as a function of particle size: 1.0–2.0 mm (red); 0.5–1.0 mm (blue) and <0.5 mm (green). Symbols of filled and empty circles were used to indicate adsorption and desorption isotherms, respectively.

Table 4. Characterization of lignite porosity as a function of particle size.

Size fraction	Pore volume (Gurvich) at p/p^0 = 0.95 (cm^3/g)	Surface area (cm^2/g)
< 0.5 mm	0.019	3.6364
0.5–1.0 mm	0.0086	3.8037
1.0–2.0 mm	0.0051	2.2167

The specific surface area of <0.5 mm and 0.5–1.0 mm lignite fractions were similar (Table 4). However, the lignite fraction with the largest particle size had the lowest surface area. This means that, grinding modified porosity of the different lignite samples. Thus, the surface area and the pore volume increased several times by decreasing the particle size. However, the surface area did not increase considerably below 1.0 mm grain size. Therefore, it can be concluded that grinding of lignite below 1.0 mm is unnecessary based on the present investigation.

The zero surface charge characteristics of the three different lignite size fractions applied in the same dose as in the incubation experiments (i.e., 5.0% by weight) has proven to be very similar. These results obtained for all three lignite fractions in a 0.01 mol/L NaCl solution are shown in Figure 7. Thus, two PZC values could be determined. No considerable shift was observed in the PZC values by varying the ionic strength of the electrolyte background (i.e., in the range of 0.001–0.1 mol/L NaCl).

Both PZC values were observed in the acidic region owing to the HA and fulvic acid content of lignite. This finding is in good agreement with previous data reported on Lakhra-coal [148], lignite particles of 0.1–0.3 mm size mined in India applied for removal of Pb(II) ions [149] and activated coal originating from the Thar coalfield in Pakistan [150]. In the present investigation, one PZC was from the environmental point of view, only the second PZC value is relevant. Thus, at pH above this second PZC, the surface of the lignite is negatively charged enhancing adsorption of Cr(III) ions, as well as its positively charged hydroxo complexes formed at slightly basic pH values.
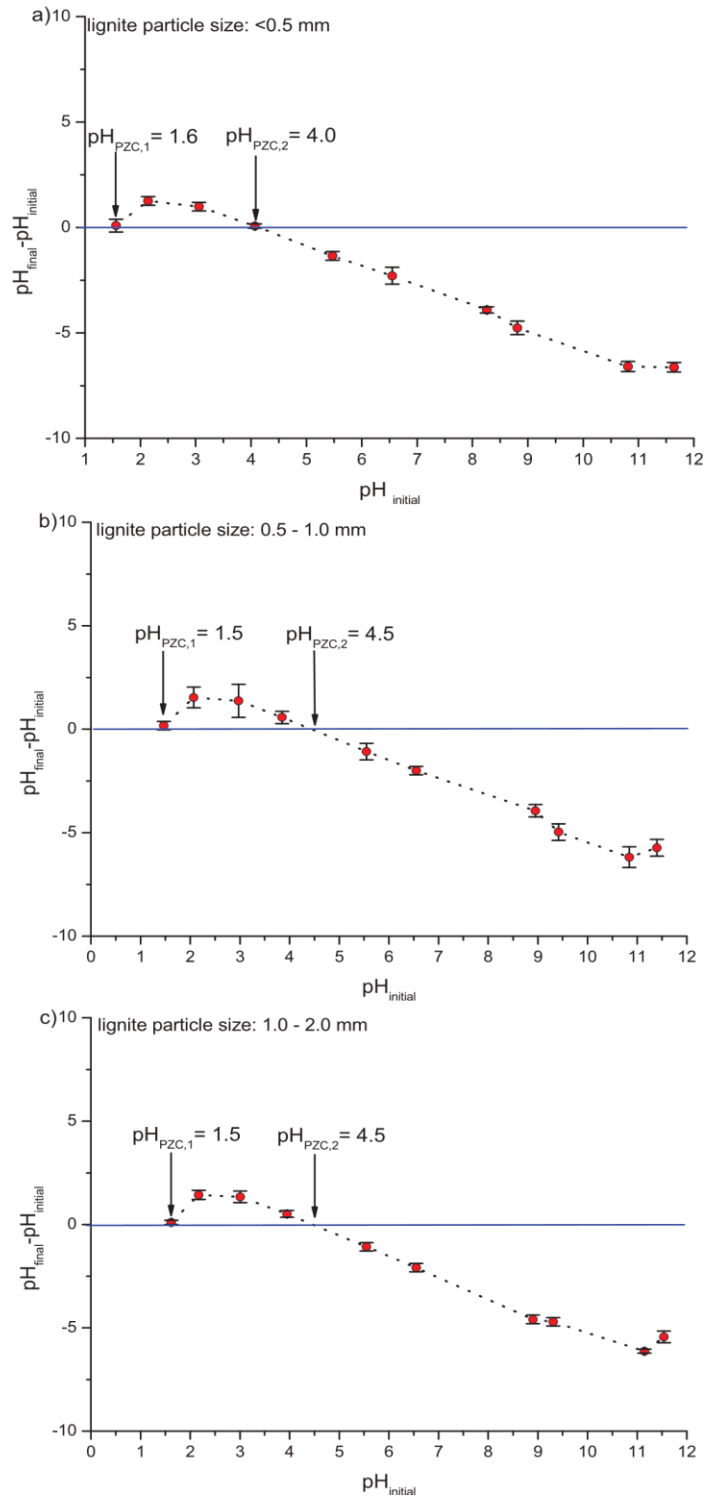
Figure 7. Point of zero charge (PZC ± standard deviation) values (n = 3) of lignite having <0.5 mm (a); 0.5–1.0 mm (b) and 1.0–2.0 mm (c) particle size ranges determined by the pH drift method. Data illustrated with dashed lines for better visualization of the PZC values.

5.1.2 Analytical capabilities and quality assurance of Cr determination

Chromium concentration in the leachates from the various extraction steps were analyzed by ICP-SF-MS. Moreover, the elemental concentration in the *aqua regia* extracts as well as in the *pseudo*total fractions were also determined by ICP-SF-MS after MW-assisted digestion with *aqua regia* cf. EU Standard EN 13346 [145]. After subtraction of the blank values, proper mass balances could be established between the sum of Cr contents in the various fractions and the corresponding *pseudo*total elemental concentrations. The set-up of the mass balance demonstrated that Cr could be effectively extracted from the artificially contaminated soils especially with *aqua regia* without necessarily applying HF which is toxic and hadardous.

Besides this technical requirement, the precision of the results expressed as the relative standard deviation of the mean Cr concentration calculated from the results of three replicates was generally less than 20% for each sample matrix.

Accuracy was checked by analyzing each representative sample matrix by an alternative instrumental analytical technique. For our investigations, TXRF was chosen as being a multi-elemental and cost-effective instrumental approach with excellent limits of detection for Cr determination. Due to the relatively high application dose of Cr in the soil coupled with the presence of the organic leaching agents as well as in the soil samples, the layer thickness of the dry residues on the TXRF sample carriers could easily be minimized by applying appropriate dilution to the sample solutions. The total Cr concentrations in the same soil sample matrices corresponding to the 0.5–1.0 mm lignite grain size fractions determined by ICP-SF-MS and TXRF have been shown on Table 5. The smallest deviation (<10%) of the concentrations obtained for Cr by the two different analytical techniques was obviously observed for samples subjected to MW-assisted digestion prior to elemental analysis. Comparable deviation values were obtained for the EDTA containing fractions diluted 1000-fold prior to TXRF analysis. Larger variations in Cr concentrations reaching in some cases as high as 30% were observed for the one hundred-fold diluted acetate- and hydroxylamine-hydrochloride-based samples. These variations did not considerably depend on the elemental concentration, but rather on the organic content of the investigated samples (Table 5). However, as it was mentioned, TXRF is a cost-effective multi-element analytical technique and hence, it can be used instead of CRM analysis without even performing MW-assisted acid digestion of the leachates.

As a recovery test, the concentration of Cr in the different leachates was summed and related to the *pseudo*total Cr concentration (Table 6). As expected, the sum of the Cr concentration in the different fractions was generally lower than the corresponding *pseudo*total concentration. Nevertheless, the deviation, with few exceptions, did not exceed +20% (Table 6).

5.1.3 Mobility reduction of iCr(III) in soils containing lignite with different particle sizes

Approximately 90% of the *pseudo*total Cr was immobilized by the calcareous sandy soil itself due to its basic pH (Figure 8a). Distribution of Cr among the different fractions showed a similar pattern independently of the treatment type and the presence or absence of lignite (Figure 8a). Moreover, the lignite particle size had little influence on Cr immobilization (Figure 8a). When the calcareous sandy soil was contaminated with Cr(III), abundance of Cr in the acetic acid and hydroxylamine leachates was generally less than 2% and 5%, respectively (Figure 8a). It is likely that positively charged Cr(III) hydroxo complex species were formed during the interaction of Cr with the calcareous soil matrix. Since the environmentally relevant PZC value was cca. 4.5, adsorption of $CrOH^{2+}$ and $Cr(OH)_2^+$ species onto the surface of the applied lignite between pH = 5 and 9 could not be neglected. However, $CrOH^{2+}$ and $Cr(OH)_2^+$ species formed in the aforementioned pH interval possess low water solubility [151]. Due to the immobilization of the Cr(III) in the form of hydroxo species formed in the calcareous soil, it can be presumed that Cr in the soil does not reach the lignite particles.

Table 5. Total Cr concentrations (n = 3) in all relevant soil sample matrices determined by means of ICP-SF-MS and TXRF

	+ 375 mg/kg Cr(III) treatment	
	concentration (mg/kg ± SD)	
Analytical technique	ICP-SF-MS	TXRF
Sample matrix	acidic soil + 0.5 – 1.0 mm ∅ lignite	
AcOH leachate	33.5 ± 2.9	41.5 ± 4.1
NH$_2$OH leachate	64.0 ± 5.8	65.5 ± 4.5
EDTA leachate	25.7 ± 2.1	23.4 ± 2.2
*pseudo*total	349 ± 9	352 ± 43
Sample matrix	alkaline soil + 0.5 – 1.0 mm ∅ lignite	
AcOH leachate	16.0 ± 2.5	16.7 ± 3.4
NH$_2$OH leachate	64.0 ± 3.8	54.0 ± 4.0
EDTA leachate	26.4 ± 2.5	26.7 ± 2.5
*pseudo*total	359 ± 7	341 ± 22

Abbreviations: ICP-SF-MS - inductively coupled plasma sector field mass spectrometry; SD - standard deviation; TXRF - total-reflection X-ray fluorescence spectrometry.

Table 6. Total Cr concentration (n = 3) for the relevant soil treatments compared to the sum of the concentrations in various leachate fractions

Soil treated with 375 mg/kg Cr in form of Cr(III)	Leaching test	Cr concentration (mg/kg ± SD)		Recovery rate (%)
		*pseudo*total	Σ fractions	
Acidic sandy soil				
+ no lignite	fit-for-purpose BCR	347 ± 8	322 ± 12	108
	phytoavailability		354 ± 6	98
+ <0.5 mm sized lignite	fit-for-purpose BCR	349 ± 9	296 ± 15	118
	phytoavailability		350 ± 4	99
+ 0.5 – 1.0 mm sized lignite	fit-for-purpose BCR	343 ± 10	352 ± 5	97
	phytoavailability		345 ± 6	99
+ 1.0 – 2.0 mm sized lignite	fit-for-purpose BCR	330 ± 12	364 ± 3	91
	phytoavailability		343 ± 8	96
Calcareous sandy soil				
+ no lignite	fit-for-purpose BCR	357 ± 7	322 ± 10	111
	phytoavailability		355 ± 4	101
+ <0.5 mm sized lignite	fit-for-purpose BCR	342 ± 6	347 ± 5	99
	phytoavailability		372 ± 2	92
+ 0.5 – 1.0 mm sized lignite	fit-for-purpose BCR	359 ± 7	324 ± 9	111
	phytoavailability		352 ± 4	102
+ 1.0 – 2.0 mm sized lignite	fit-for-purpose BCR	377 ± 8	320 ± 11	118
	phytoavailability		364 ± 3	104

Abbreviations: BCR – Community Bureau of Reference; SD – standard deviation.

On average, a 20% lower immobilization rate was recorded for acidic control soil, compared to that obtained for the calcareous soil without the addition of lignite due to the hydroxylamine extraction applied (Figure 8b). The Cr content of the hydroxylamine leachate increased by about 10-20% upon the addition of lignite. Nevertheless, the addition of lignite contributed to the reduction of Cr mobility in the acetic acid leachates presumably due to immobilization through binding to cation-exchange sites of lignite. This finding was corroborated by the fact that the pH of the acidic soil used is 5.0 and the environmentally relevant PZC value of the lignite samples was at pH ≈ 4.5. Nevertheless, the immobilization rate of Cr in acidic soil was again not influenced by the lignite size fractions. In the case of the acidic soil, hydrolysis of iCr(III) is less pronounced, and hence iCr(III) mobility increases. Similar findings by Pukalchik et al. [152] suggest that solution pH values can significantly affect metal species distribution and, as a result, metal sorption in soil. Changes in pH influence directly humic products, because of their functional groups such as; carboxyl, phenolic, and amino are pH-dependent [152], which may result in Fe(III) reduction to Fe(II) [153].

Upon addition of lignite to the acidic soil artificially contaminated with iCr(III), Cr availability decreased by about 10% in the hydroxylamine leachates independently of the lignite particle size applied. The hydroxylamine hydrochloride solution (pH=2) reduces most of Fe(III)/Mn(IV). The mean concentration of Fe and Mn in the investigated soils can be seen in Table 1. Iron was released in less than 1% in the acetic acid extracts. However, the Fe abundance in the samples after leaching with hydroxylamine was about 5% of the *pseudo*total Fe independently of the type of soil or treatment type. At the same time, the concentration of Mn in different leachates were below the limit of quantitation after leaching and MW-assisted acid digestion.
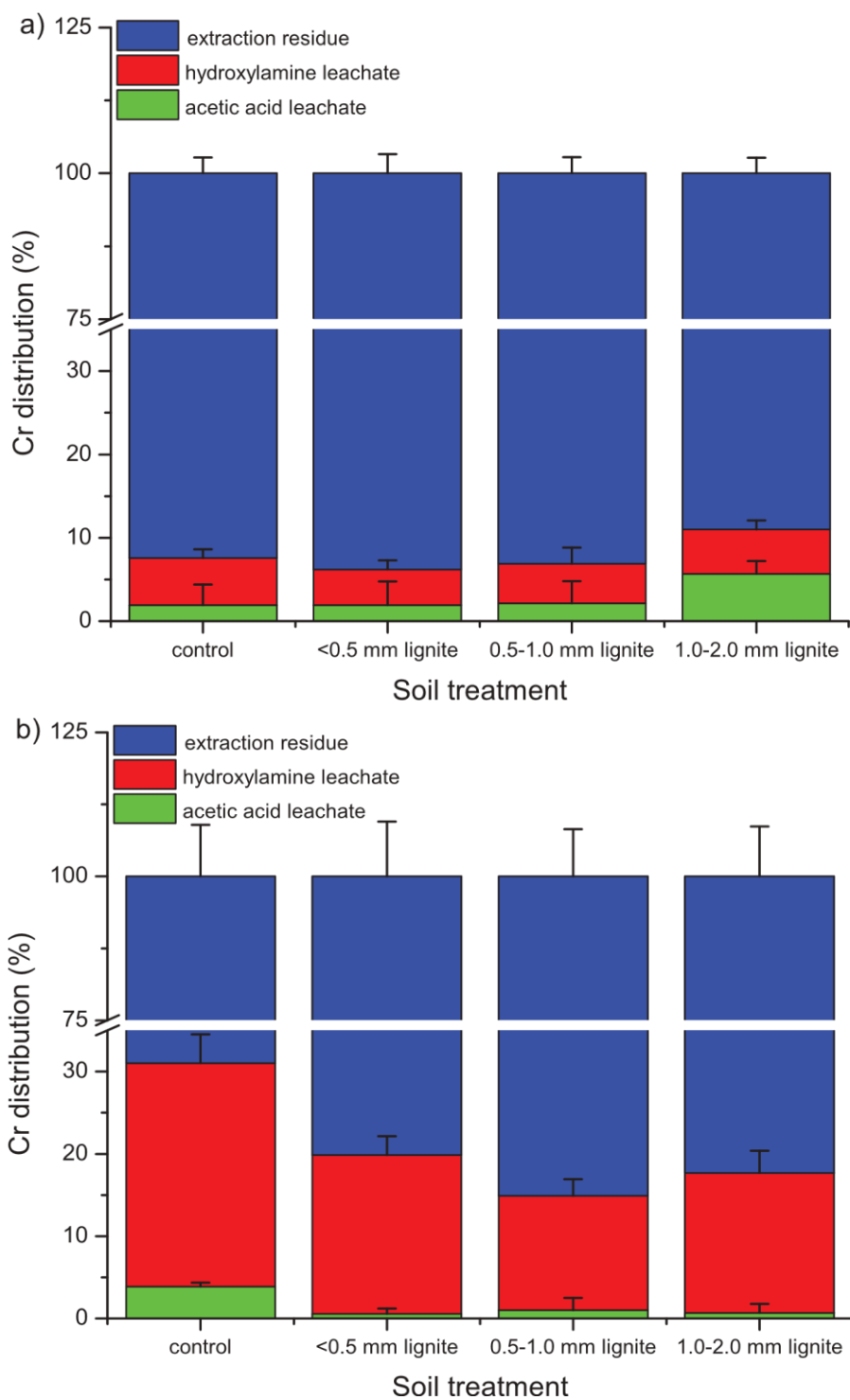
Figure 8. Chromium distribution (%) among different leachates of calcareous (a) and acidic (b) sandy soils without lignite or containing 5.0% lignite by weight and particle size ranges of <0.5 mm; 0.5–1.0 mm or 1.0–2.0 mm after eight weeks of incubation with 375 mg/kg Cr(III). Residual percentage originated from individual measurements.

5.1.4 Assessment of phytoavailability in soils artificially contaminated with iCr(III)

Concerning the assessment of the phytoavailability of the investigated elements, EDTA is widely used extractant. Nevertheless, complexation of iCr(III) is hindered due to the thermodynamic stability and inertness of its aquo complex species. However, the use of a single extractant is always advantageous from the viewpoint of measurement uncertainty. According to the present results, the phytoavailable Cr fraction estimated by leaching of the calcareous soil with EDTA was about 10–20% of the *pseudo*total Cr independently of the applied treatment (Figure 9a). Again, the soil alkalinity (i.e., pH ≈ 8) and the CEC of lignite immobilized iCr(III) through hydrolysis and subsequent formation of low water-solubility positively charged hydroxo complexes, respectively.

In the case of the acidic soil, approximately 20–25% of the *pseudo*total Cr concentration was leached from the control and from the <0.5 mm lignite particle size treatment, while the phytoavailable Cr fraction decreased to about half this value, when lignite particle size was 0.5–1.0 mm and 1.0–2.0 mm (Figure 9b). According to our results, Mn could not be again quantified in the case of EDTA extraction and approximately, 2–3% of the *pseudo*total Fe could be determined independently of the soil pH and type of treatment.

Assuming that the higher plants are capable of nutrient uptake by root surface acidification often accompanied by H^+-mediated reduction, leaching with hydroxylamine can be considered to a certain extent suitable for the estimation of phytoavailable fraction of Cr, especially, because EDTA is not capable of complexing iCr(III) at ambient temperatures, due to kinetic hindrance. Therefore, it seems reasonable to compare the percentage of Cr in EDTA and hydroxylamine leachates. The hydroxylamine and EDTA leachates gave similar results for both soils and lignite addition. Thus, the stabilization patterns of Cr as a function of the lignite particle sizes were in agreement. The only difference was that the Cr percentage in the hydroxylamine leachate of the calcareous soil was about twice less than in the corresponding acidic soil leachates. The EDTA seems to liberate Cr indirectly through complexation of other metal ions. In return, hydroxylamine liberates iCr(III) associated to amorphous Fe(III)/Mn(IV) minerals through the reduction of these two latter elements. Due to the low pH of this reducing agent (pH= 2), the relatively mobile Cr in acidic soil can be retained by the lignite particles.
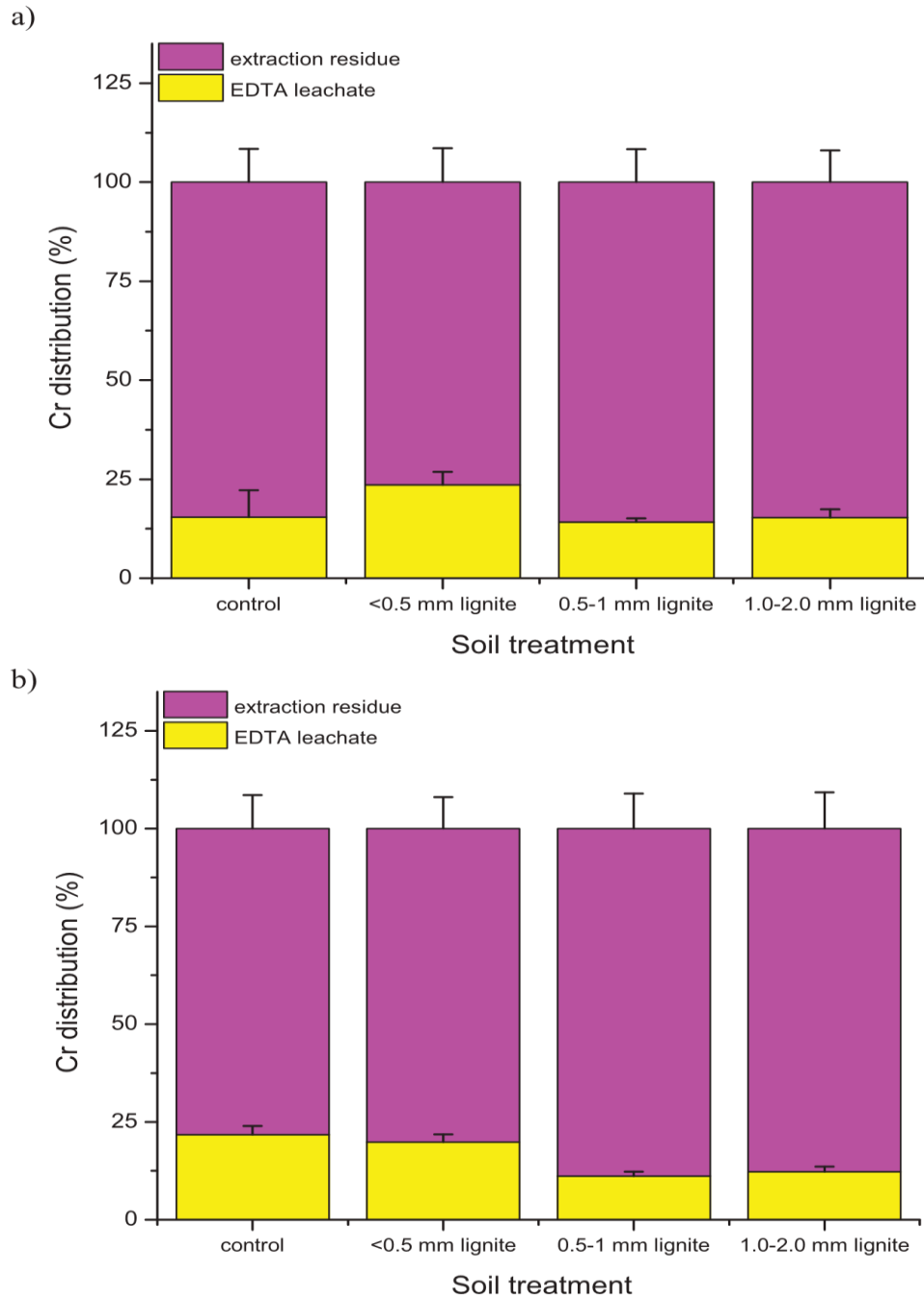
Figure 9. Chromium distribution (%) between the EDTA leachates and extraction residue of calcareous (a) and acidic (b) sandy soils without lignite or containing 5.0% lignite by weight and particle size ranges of <0.5 mm; 0.5–1.0 mm or 1.0–2.0 mm after eight weeks of incubation with 375 mg/kg Cr(III). Residual percentage originates from individual measurements.

5.2 Granular activated charcoal prepared from peanut (*Arachis hypogea*) shell for mobility reduction of arsenate in soil

5.2.1 Quality assurance of arsenic determination

Quality assurance for soil chemical analyses is a key issue considering the heterogeneity of the samples. The use of ICP-SF-MS for As determination even at a soil dosage of 15 mg/kg iAs(V) representing the permissible total As concentration according to the Hungarian legislation in force [6/2009. (IV. 14.), KvVM-EuM-FVM,2009] [154] ensured excellent detection limits and dynamic range for quantitative determination. Besides the relatively large As concentration in the samples, the high resolution mode of the ICP-SF-MS eliminates the problems that arise as a result of the molecular interference of $^{40}Ar^{35}Cl^+$ on the signal of $^{75}As^+$ especially occurring due to the *aqua regia* digestion and soil leached with hydroxylamine hydrochloride. Therefore, in the present work, special attention was paid to the procedural blanks, precision, recovery and accuracy of the results.

All blank combinations were taken into account and there was no quantifiable As in the analyzed blank samples. Therefore, proper mass balances could be set up and As distribution among the different leachate fractions could be established. The precision expressed as the relative standard deviation of the measurements performed in triplicates were < 20% either for the individual samples (Table 7) as well as for the different leachate fractions (Figure 10).

Compared to the nominal value of 15 mg/kg and 30 mg/kg, the mean of the *pseudo*total As concentrations were 15.4 ± 1.9 mg/kg and 29.9 ± 1.7 mg/kg, respectively. Among the concentration data obtained at the lower As concentration treatment, the minimum and maximum concentration values differed approximately by ± 15% from the nominal value (Table 7). As a recovery test, the concentration of As in the different leachate fractions were summed and related to the *pseudo*total As concentration (Table 7). As expected, the sum of the As concentration in the different fractions were generally lower than the corresponding *pseudo*total concentration. Nevertheless, the deviation, with few exceptions, did not exceed +20% (Table 7). Additional sample manipulation with OA caused lower *pseudo*total As concentration compared to the sum of the fractions (Table 7).

Table 7. Total As concentration (n=3) for the relevant soil treatments compared to the sum of the concentrations in the various leachate fractions

Soil treated with 15 mg/kg As in form of iAs(V)	Leaching test	As concentration (mg/kg ± SD)		Recovery rate (%)
		*pseudo*total	Σ fractions	
+ ∅	fit-to-purpose BCR	17.3 ± 1.4	14.1 ± 0.2	123
	phytoavailability		13.1 ± 0.1	132
+ cc. HNO$_3$-AC	fit-to-purpose BCR	12.8 ± 0.7	12.6 ± 0.2	102
	phytoavailability		12.7 ± 0.4	101
+ Celite®-AC	fit-to-purpose BCR	15.5 ± 1.1	13.4 ± 0.5	116
	phytoavailability		13.3 ± 0.1	117
+ Florisil®-AC	fit-to-purpose BCR	16.7 ± 0.2	14.2 ± 0.1	118
	phytoavailability		14.1 ± 0.6	118
+ OA/soil	fit-to-purpose BCR	13.5 ± 1.7	14.9 ± 1.7	91
	phytoavailability		15.4 ± 0.2	88
+ OA/soil + Florisil®-AC	fit-to-purpose BCR	16.6 ± 0.1	14.2 ± 0.1	117
	phytoavailability		14.1 ± 0.6	118

AC = activated charcoal; BCR = Community Bureau of Reference; OA = oxalic acid.

To check the accuracy of the results, concentration data obtained by ICP-SF-MS for sample sets corresponding to all type of soil treatment combinations at the lower AC application rate and iAs(V) dosage were compared with TXRF measured concentrations. Since high organic matrix constituent concentration of some leachates can affect the reliability of the results from TXRF analysis, the highest but optimum dilution factors were applied to these samples ensured RSD values of < 10%. Moreover, the volume of samples dropped onto the quartz carrier plates was doubled as compared to the usual value to increase the quantifiable amounts of As. The results obtained by the two analytical techniques for relevant sample matrices were in good agreement (Table 8).

Table 8. Quality assessment of the As concentration data (n=3) for all combinations of soil treatments by means of ICP-SF-MS and TXRF

	As concentration (mg/kg)		
Acidic sandy soil + 15 mg/kg As in form of iAs(V)			
Fraction	ICP-SF-MS	TXRF	Deviation (%)[*]
AcOH leachate	8.76 ± 0.24	7.58 ± 0.76	+16
NH$_2$OH leachate	2.91 ± 0.02	3.23 ± 0.48	-10
Extraction residue	2.38 ± 0.09	2.85 ± 0.22	-16
Σ fractions	*14.1*	*13.7*	
EDTA leachate	6.90 ± 0.04	6.30 ± 1.15	+10
EDTA extraction residue	6.29 ± 0.06	6.01 ± 0.50	+5
Σ fractions	*13.2*	*12.3*	
*pseudo*total	17.3 ± 0.1	14.9 ± 2.0	+16
Acidic sandy soil + 15 mg/kg As in form of iAs(V) + 2 wt% granular activated charcoal			
AcOH leachate	5.09 ± 0.22	4.90 ± 0.76	+4
NH$_2$OH leachate	3.70 ± 0.38	3.80 ± 1.04	-3
Extraction residue	3.90 ± 0.43	3.45 ± 0.55	+13
Σ fractions	*12.7*	*12.2*	
EDTA leachate	4.21 ± 0.05	4.56 ± 1.16	-8
EDTA extraction residue	8.22 ± 0.36	7.90 ± 0.70	+4
Σ fractions	*12.4*	*12.5*	
*pseudo*total	12.4 ± 0.1	12.9 ± 2.0	-4
Acidic sandy soil + 15 mg/kg As in form of iAs(V) + 2 wt% granular AC + 0.01 M OA			
Fraction	ICP-SF-MS	TXRF	Deviation (%)[*]
AcOH leachate	5.08 ± 0.12	4.26 ± 0.64	+19
NH$_2$OH leachate	4.42 ± 0.28	4.16 ± 1.20	+6
Extraction residue	4.23 ± 0.3	3.83 ± 0.41	+15
Σ fractions	*13.7*	*12.3*	
EDTA leachate	5.26 ± 0.16	5.43 ± 1.05	-3
EDTA extraction residue	8.57 ± 0.48	7.98 ± 0.50	+7
Σ fractions	*13.8*	*13.4*	
*pseudo*total	12.3 ± 1.0	10.2 ± 1.5	+20

* expressed as concentration of As by ICP-SF-MS divided by the one by TXRF (%). AC = activated charcoal; OA = oxalic acid.

5.2.2 Application of a fit-for-purpose BCR extraction procedure for evaluation of As distribution in different peanut shell derived charcoal amended acidic soil

In the case of the SAs$_{15}$AC$_0$ and SAs$_{30}$AC$_0$ treatments (Table 2) only ≈15% of the iAs(*V*) dose was retained after one month incubation with As (Figure 10a). Since soil matrices can be very complex, a relatively simple soil of acidic pH with low OM, high silt and clay contents was

chosen to be able to interpret the mobility reduction processes studied. Due to the fact that the prevalent As species in the upper soil layers is iAs(V), dihydrogenarsenate ions were chosen to artificially contaminate the acidic sandy soil sample. To a first approximation, the iAs dose corresponding the permissible value for total As in soil in Hungary [6/2009. (IV. 14.), KvVM-EuM-FVM,2009] [154] has been considered for the treatments.

By adding granular AC prepared from peanut shells to the soil samples in application rate of 2 wt%, the following order could be established for As mobility reduction according to As distribution among the different fractions at a 15 mg/kg iAs(V) dosage: $SAs_{15}AC_0 < SAs_{15}Celite-AC_2 < SAs_{15}AC_2 \approx SAs_{15}Nitric-AC_2 \approx SAs_{15}Florisil-AC_2$. The similar As immobilization rates obtained for $SAs_{15}AC_2$, $SAs_{15}Nitric-AC_2$ and $SAs_{15}Florisil-AC_2$ indicated that Florisil$^®$ mainly played the role in the mechanical stabilization of the AC. It should be emphasized hereby, that the reference AC was dusty and an additional loss of approximately 15 wt% after sieving through a < 2 mm mesh size sieve before mixing with the soil was observed, while there was practically no loss (< 1.2 wt%) by sieving the Florisil$^®$-modified AC. However, the differences between the As percentage in the fraction originating from the soil amended with different peanut shell derived AC materials were not considerable, registering 5–10%, on average (Figure 10a). A much more considerable difference in As immobilization, however, could be observed by comparing the As distribution between the $SAs_{15}AC_0$ and $SAs_{15}Florisil-AC_2$ treatments Thus, $SAs_{15}Florisil-AC_2$ treatment was capable of reducing As mobility 20% more than the the $SAs_{15}AC_0$ one (Figure 10a).
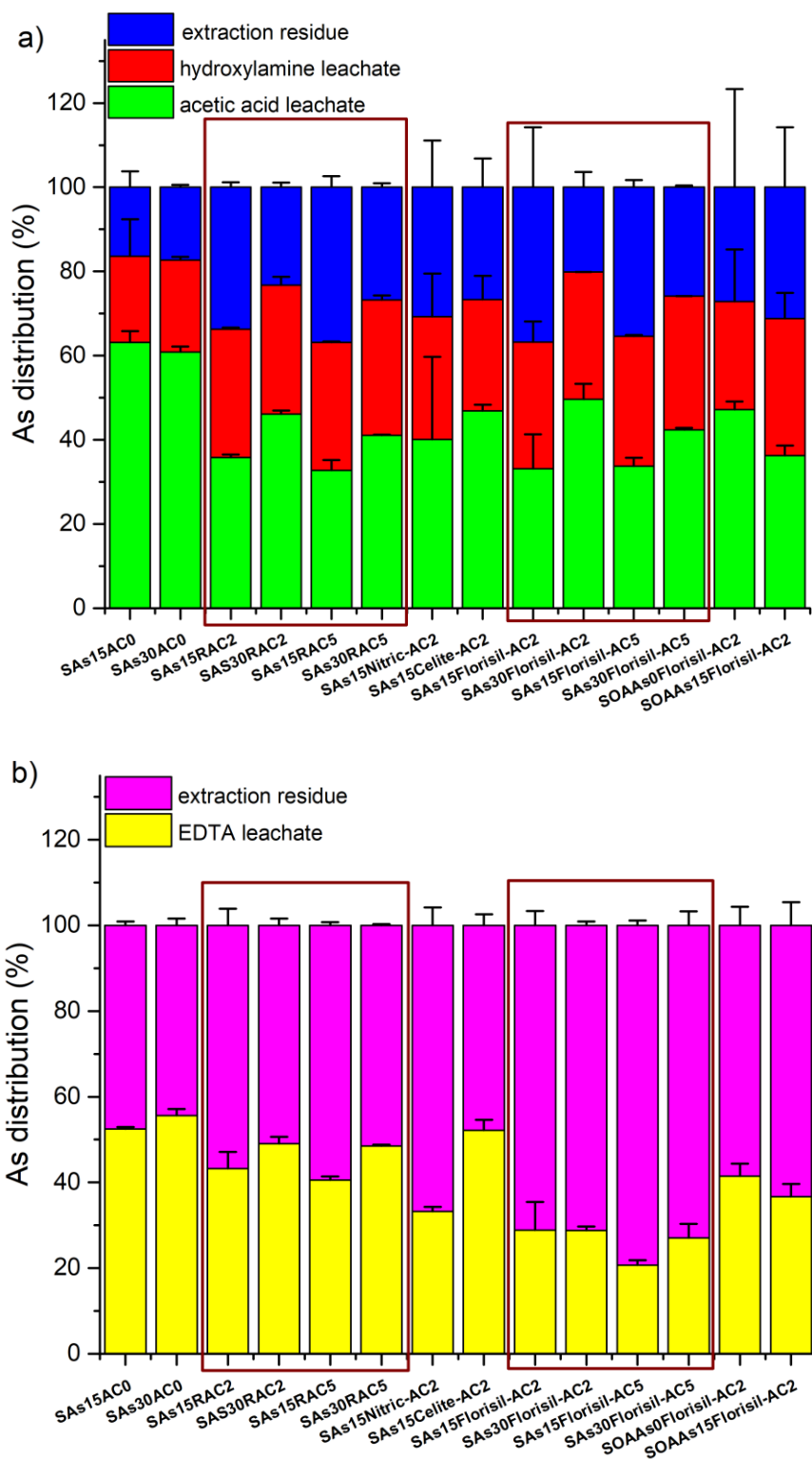
Figure 10. Arsenic distribution (%) among the fractions obtained after performing fit-to-purpose BCR leaching (a) and phytoavailability (b) tests. Error bars represent the relative standard deviation (%) of the calculated data (*n*=3). Abbreviations: AC=activated charcoal; OA=oxalic acid.

A much higher (i.e., about 30%) immobilization capacity was achieved by $SAs_{15}Florisil-AC_2$ treatment when comparing the As content of the acetic acid leachate in the $SAs_{15}AC_0$ and $SAs_{15}Celite-AC_2$ and $SAs_{15}Nitric-AC_2$ treatments. Although peanut shell is common and cheap, the application rate to the soil in the form of AC was kept as low as possible due to large differences in dissolved organic and phosphate contents, pH and CEC large variations have been observed in the literature for As mobility in soil [155]. The optimum BC application in arable land has been suggested to be between 1% and 5% [156]. However, $SAs_{30}Florisil-AC_5$ treatment was also performed as being the most promising among all treatments. In order to compare the outcomes of these additional treatments, similar experiments were conducted, namely $SAs_{15}RAC_5$, $SAs_{30}RAC_2$ and $SAs_{30}RAC_5$. Thus, similar percent values were obtained for $SAs_{15}RAC_2$, $SAs_{15}RAC_5$, $SAs_{15}Florisil-AC_2$, $SAs_{15}Florisil-AC_5$ and as well as $SAs_{30}RAC_2$, $SAs_{30}RAC_5$, $SAs_{30}Florisil-AC_2$ and $SAs_{30}Florisil-AC_5$ treatments (Figure 10a). Deviation in these results obtained did not exceed 20%. However, the amounts of As that could be immobilized increased almost proportionally when the AC application rate was increased and the iAs(V) dosage was doubled.

Silicate containing common additives – diatomaceous earth and magnesium metasilicate launched under the brand names of Celite® and Florisil®, respectively - have also been used with the primary aim of increasing the mechanical stability of the AC materials derived from peanut shell. Although Celite® cannot participate in ion-exchange processes due to its chemical composition, the rationale behind its application was that its silanol groups may form hydrogen bonds with iAs(V). In addition, Florisil® is a widely accepted adsorbent in chromatography (hence, primarily for polar organic compounds). Built up by discrete $MgSiO_3$ units, it is believed to form hydrogen bonds with iAs(V) or OA. By comparing the As mobility reduction performance of the AC materials further modified with Celite® and Florisil®, the main difference relies in the structure of these two additives. Thus, the former is an inert and untreated diatomaceous earth composed mainly of amorphous SiO_2 with less surface Si-OH groups [157], while the latter is characterized by discrete trisilicate ion blocks even in the bulk region capable of adsorption of oxyanions [158]. Presumably, the hydroxyl groups of Florisil® bind the carboxylic groups of the AC more efficiently, rendering a mechanically stable granular presentation less prone to diffusion.

The mobility reduction capacity of the $SAs_{15}Florisil-AC_2$ treatment was about 10% less compared to the As percentage in the easily reducible fraction extracted by hydroxylamine in the reference soil matrices (Figure 10a) for both iAs(V) dosages. The other soil samples amended with different charcoal materials showed a similar behavior, namely, the As percentage in the hydroxylamine fractions was again about 10% larger than the As determined in $SAs_{15}AC_0$ treatment. The higher plants are capable of nutrient uptake by root surface acidification often accompanied by H^+-mediated reduction. In this way, reduction of the hardly water-soluble Fe(III) compounds to the more water- and acid soluble Fe(II) compounds have been described [159]. At the same time, reduction of iAs(V) to iAs(III) requires strong and concentrated acid solutions [160]. The resulting iAs(III) is a weak acid of $pK_{a1} \approx 9.2$. Therefore, iAs(III) can mainly be found in undissociated form in the pH range of our experiments. In return, electrically neutral species would have been stabilized at a larger extent by the AC materials used (e.g. through formation of hydrogen bonds). The $\pm$ 10% differences in the As percentage value of the hydroxylamine leachates independently of the treatments applied are within the margin of error and, therefore, they do not support the considerable reduction of iAs(V) to iAs(III).
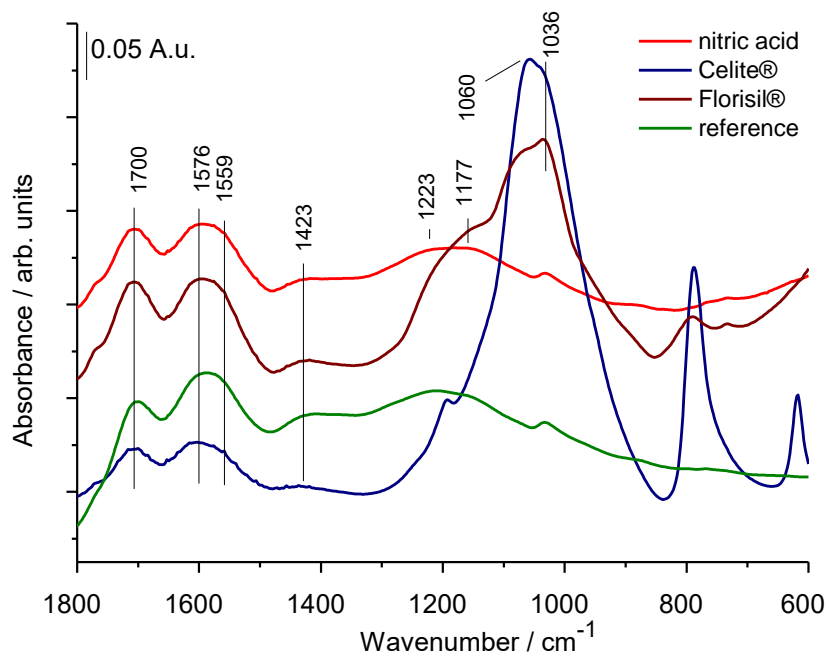
The ATR-FT-IR measurements demonstrated the presence of carboxylate groups (Figure 11a) attached to aromatic rings (Table 9) in all three AC modifications. Moreover, C=O bands of carboxylic groups and as part of unconjugated aldehydes/ketons could also be assigned for all three materials (Table 9). However, C-O bonds in esters, phenols and alcohols could be only detected in the sample functionalized with HNO_3. The lack of this assignment in the silica modified charcoal materials might be due to the overlap represented by the large vibrational band of Si-O-Si groups (Figure 11a). Large H-bonded OH bands could be detected in all three AC samples (Figure 11b). Again, C-OH groups could be unambiguously assigned only to the chemically functionalized AC (Table 9) due to the large Si-O-Si vibrational band registered for the silica modified materials (Figure 11b). Small differences between the differently activated samples are observable in the subtracted spectra using the spectrum of the ground peanut shell treated with cc. sulfuric acid as subtrahend spectrum (Figure 11c). The most intriguing part of the spectra is restricted to the 1800–1300 cm^{-1} wavenumber region where characteristic stretching vibrations of carboxylates, carbonates and carbonyls etc., appear (Figure 11c). An additional characteristic vibrational band corresponding to carboxylates could be assigned only to the Florisil®-AC after subtraction of the reference spectrum at 1554 cm^{-1} (Figure 11c). At

50

higher wavenumbers, only some excess of water can be observed for the HNO$_3$ charcoal. Low temperature chars with low aromaticity contain more C=O and C–H groups that promote adsorption of contaminants [161]. Many BCs tested for As removal are low temperature derived (300–500 °C) as the presence of more functional groups encourages a better adsorption of HM(loid)s as compared to BCs derived at higher temperature [155].

Table 9. Infrared absorption bands (cm^{-1}) and possible assignments

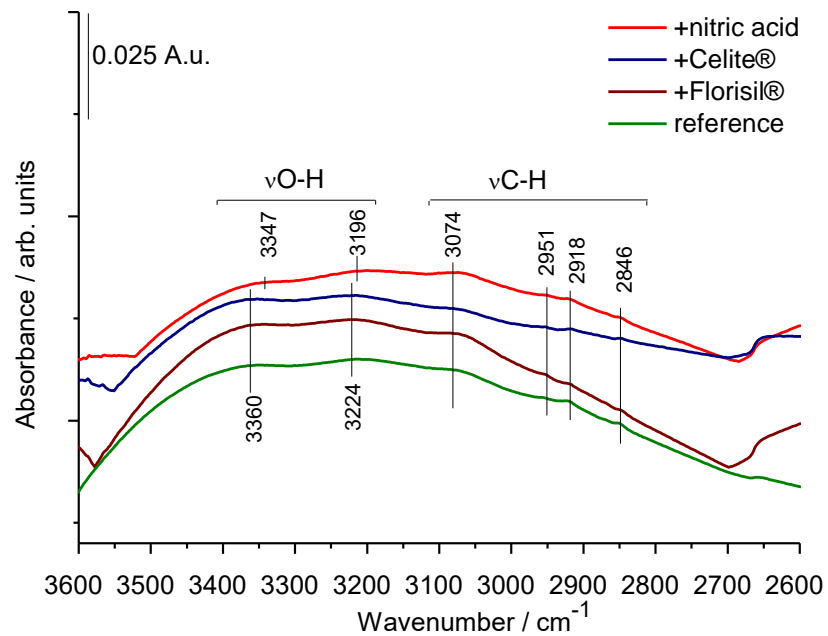| Charcoal			Assignment
+HNO$_3$	+Celite®	+Florisil®	
Absorption bands (cm^{-1})			
3347	**3360**	**3360**	**ν(-OH), H-bonded**
3196	**3224**	**3224**	
3074	3074	3074	ν(C-H), aromatic
2951	2951	2951	ν(C-H), aliphatic
2918	2918	2918	
2876	2876	2876	
1769/1175	**1769/1775**	**1769/1767**	**νC=O, unconjugated aldehydes/ketons**
-	**-**	**1730**	**νC=O, benzoate esters**
1709	**1709**	**1709**	**νC=O, carboxylic group**
1634	**1634**	**-**	deformation vibration of water
-	**1610**	**1610**	**ν$_{as}$COO$^-$**
-	**-**	**1554**	**ν$_{as}$HCO$_2^-$**
1508	**1508**	**-**	**ν$_{as}$COO$^-$**
1575	**1575**	**1575**	**ν$_{as}$COO$^-$ + νC=C, aromatic ring**
1559	**1559**	**1559**	**ν$_{as}$COO$^-$**
1471	**1471**	**1471**	**ν$_s$COO$^-$**
1423	**1423**	**1456**	**ν$_s$COO$^-$**
1223	**-**	**-**	**νC-O, esters/phenols/alcohols**
1177	**-**	**-**	
-	*1060*	*1060*	*νSi-O-Si*
-	*1036*	*1036*	
1031	**-**	**-**	**νC-OH**
-	*788*	**-**	*νSi-OH*

a)

b)

Figure 11 a&b. ATR-FT-IR spectra of granular activated charcoal varieties made of peanut ground shell treated with cc. sulfuric acid (reference); nitric acid charcoal; Celite®-charcoal and Florisil®-charcoal indicating vibrational bands due to the presence of carboxylic (a) and hydroxyl groups (b)
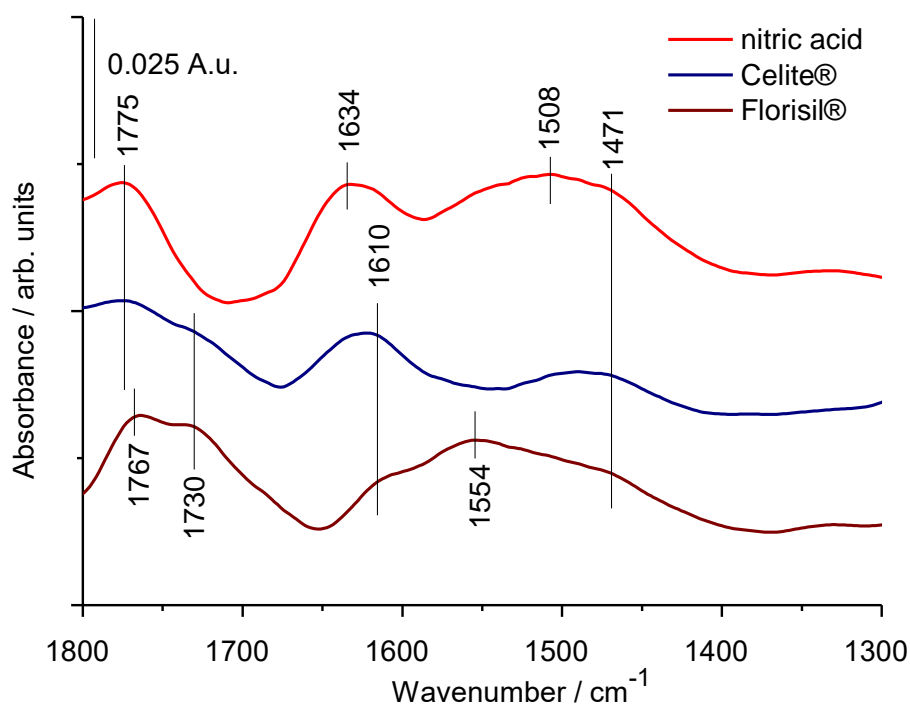
c)

Figure 11c. ATR-FT-IR spectra of granular activated charcoal varieties made of peanut ground shell treated with cc. sulfuric acid (reference); nitric acid charcoal; Celite®-charcoal and Florisil®-charcoal indicating characteristic stretching vibrations of carboxylates, carbonates and carbonyls after subtracting the reference spectra

Another approach for protonation of iAs(V) and carboxylate ions of the charcoal matrix was explored by soaking the samples with OA. Although OA itself does not belong to the Krebs cycle, oxaloacetate from the Krebs cycle can be hydrolyzed to oxalate and acetate e.g. in fungi and excreted into the soil [162]. Thus, OA can be quite common is soil systems, and it possesses the highest acid dissociation constant as compared to common Krebs cycle acids such as citric, malic or fumaric acids. Thus, an additional 10% of total As could be retained by the SOAAs$_0$Florisil-AC$_2$ treatment (Figure 10a). Therefore, it was confirmed that OA cannot protonate the carboxylate ions of the fulvic and HAs of the investigated soil. According to Alozie et al. [163], the surface of BC was protonated in the presence of citric acid, OA and malic acid at a molar concentration of 0.01 M, which disfavored adsorption of the cationic metals released from the soil by organic acid-driven mobilization. The choice of OA was due to its relatively high acidic strength among organic acids and hence, its ability to protonate charcoal surfaces

[163]. The SOAAs$_{15}$Florisil-AC$_2$ treatment did not result in further gain in terms of As mobility reduction in the presence of OA. This modified charcoal was chosen from the AC materials for this additional experiment because carbonization of ground peanut shell with Florisil® resulted in the largest particles and the granules obtained did not show any dispersability. Since the majority of plant origin biomass are cation exchangers and the prevalent As species in the upper soil layers is an oxyanion, further ways to increase the number of the carboxylic functional groups and to suppress the acid dissociation in the charcoal matrix as well as that of iAs(V) were considered. That is why the AC was further treated with OA. The rationale behind the use of cc. HNO$_3$ was to oxidize the hydroxyl functional groups of this matrix in order to increase the number of carboxylic groups. However, treatment with cc. HNO$_3$ decreased at the largest extent the charcoal mass.

In summary, OA, as being a medium strength acid considering its first acid dissociation constant was not capable of promoting protonation of iAs(V) and/or that of the carboxyl and hydroxyl groups of the applied AC. The charcoal matrix seemed to be somewhat protonated, since the pH of the filtrates of the OA treated soil in the absence and presence of AC were 3.00 ± 0.03 and 3.7 ± 0.04, respectively. Nevertheless, a large-scale implementation of such soil acidification treatments would have been difficult to be achieved.

5.2.3 Application of extraction with EDTA for evaluation of As mobility reduction in acidic soil amended with different peanut shell-derived charcoal materials

Since EDTA is not capable of forming coordination compound with iAs(V) but with cations such as Fe(III), this latter ion governing iAs(V) availability in the soil, the Lakanen–Erviö leaching test [144] can provide an indirect information on the possible uptake of iAs(V) by plants. However, EDTA is a relatively universal extractant allowing (in)direct determination of many elements.

The As distribution between the EDTA leachate and extraction residue was very similar for the reference (i.e. SAs$_{15}$AC$_0$, SAs$_{30}$AC$_0$, SAs$_{15}$RAC$_2$, SAs$_{15}$RAC$_5$ and SAs$_{30}$RAC$_5$) and SAs$_{15}$Celite-AC$_2$ treatments (Figure 10b). In return, in the case of the SAs$_{15}$Nitric-AC$_2$ and SAs$_{15}$Florisil-AC$_2$ treatments about 75% of total As could not be leached (Figure 10b). Compared with the reference soil (i.e. SAs$_{15}$AC$_0$, SAs$_{30}$AC$_0$) as well as reference AC-amended

soil (i.e. $SAs_{15}RAC_2$, $SAs_{15}RAC_5$ and $SAs_{30}RAC_5$) treatments, a gain of about 25% and 15% was achieved for the amendment $SAs_{15}Florisil-AC_2$ and $SAs_{30}Florisil-AC_2$ (Figure 10b), respectively. Thus, an increase of 5 wt% AC application rate gave similar results with respect to the As distribution for the Florisil®-modification compared to the 2 wt% AC application rate for both iAs(V) dosages (Figure 10b). Again, the amounts of the non-phytoavailable As is approximately double at the higher iAs (V) dose.

Again, the additional $SOAAs_{15}Florisil-AC_2$ treatment improved the mobility reduction <20% due to the hindrance of As phytoavailability modeled with EDTA extraction compared to results obtained for the reference soil treatment. Additionally, like the results from the fit-for-purpose BCR extraction [143], the $SOAAs_{15}Florisil-AC_2$ amendment did not show any beneficial effect (Figure 10b). This outcome reinforces reason for abandoning such soil experiments.

Assuming that, the higher plants are capable of nutrient uptake by root surface acidification often accompanied by H^+-mediated reduction, soil leaching with hydroxylamine can be considered to a certain extent suitable for the estimation of the phytoavailable fraction of As, especially because EDTA is not capable of complexing iAs(V). Therefore, it seems reasonable to compare the As percentages in the EDTA and hydroxylamine leachates. Thus, the former values were larger by about 30% than the latter values for the reference (i.e. $SAs_{15}AC_0$, $SAs_{30}AC_0$, $SAs_{15}RAC_2$, $SAs_{15}RAC_5$, $SAS_{30}RAC_2$, $SAs_{30}RAC_5$) and $SAs_{15}Celite-AC_2$ treatments (Figures 10 a&b). However, comparable values were obtained in both fractions for the $SAs_{15}Florisil-AC_2$, $SAs_{15}Florisil-AC_5$, $SAs_{30}Florisil-AC_2$, $SAs_{30}Florisil-AC_5$ treatments (Figures 10 a&b) (when applicable). Nevertheless, the water-soluble and carbonate-bound As fraction was removed prior to the hydroxylamine hydrochloride extraction.

5.2.4 Adsorption mechanism of iAs(V)

By plotting the corresponding c_e and q_e data pairs after loading the two most promising AC varieties (i.e., modifications with HNO_3 and Florisil®) as well as the reference AC with iAs(V) in varying concentration at the pH of the soil, almost linear relationship between the plotted data sets could be observed in the 50 to 400 mg/kg iAs(V) concentration range (results not shown) for each AC variety. In order to reveal the adsorption mechanism of iAs(V) onto the prepared AC, Langmuir and Freundlich isotherm models were considered (Figure 12). As expected, adsorption

of As could be adequately modeled with the Freundlich isotherm and not by Langmuir model in all cases after linear fitting of the proper data sets. This outcome is not surprising due to the several restrictions of the Langmuir model compared to the more permissive and empirical Freundlich model. Thus, contrary to the Langmuir model, assumptions allowing adsorption according to Freundlich include heterogeneous distribution of the binding sites, simultaneous presence of different functional groups, formation of multilayers, and covalent binding of the adsorbate [164]. The AC used in the present study fulfills all these requirements. However, differences were registered in the extent of iAs(V) adsorption from the model solutions proved by the exponent of the Freundlich equation expressed as the reverse of the slope of the linear fittings. Thus, a decrease could be established for the slopes obtained for the reference, HNO$_3$- and Florisil$^®$-modified AC varieties at pH = 5 in this order (Figures 12 a-c). However, these exponent values were close to the unit in each case indicating only a slight deviation from linearity. Hence, the largest As adsorption rate could be attributed to the Florisil$^®$-modified AC at pH = 5 (Figure 12 c). By repeating this series of experiments with this latter AC variety at pH = 8, however, the adsorption rate of As decreased (Figure 12 d) being similar to that obtained for the HNO$_3$ modification. This led to hypothesis that, adsorption of As to the AC is achieved by formation of a covalent bond between iAs(V) and O of the carboxylic functional group of the AC with simultaneous elimination of a water molecule (Eq. 3).

$$Res - COOH + H_2AsO_4^- \rightarrow Res - COO - HAsO_3^- + H_2O \text{ (Eq. 3)}$$
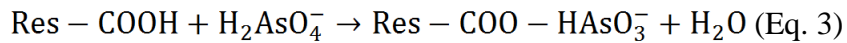
This mixed acid anhydride formation through water elimination is not favored at alkaline pH values (Eq. 4):

$$Res - COO^- + HAsO_4^{2-} \rightarrow \emptyset \text{ (Eq. 4)}$$
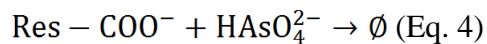
Considering protonation of the charcoal and the iAs(V) species at acidic and alkaline pH values, these very simplified approaches can be proposed.

Loading of Florisil$^®$-AC with iAs(V) at pH = 5 led to an enhancement of stretching bands related to C=O (1769, 1709 cm^{-1}), COO$^-$ (1603, 1432 cm^{-1}) and C—O (1223, 1177 cm^{-1}) and C-OH (1031 cm^{-1}) (Figure 13). Moreover, the slight wavenumber shift of the v_{as}COO$^-$ and v_sCOO$^-$ at 1603 and 1432 cm^{-1}, respectively, compared to the treated charcoal further strengthen the hypothesis that As interacts with the COO$^-$ groups (Figure 13). The increase in C=O and C—O intensities suggests that a monodentate coordination might have occurred (C(=O)-O—).

Furthermore, the weak new bands at 839 and 743 cm^{-1} could be assigned to As—O vibrations. As a comparison, the spectrum of KH_2AsO_4 has also been presented (Figure 13). Indeed, the As—O bands appeared at 856 and 749 cm^{-1}, respectively. The small shift in the case of Florisil®-modification loaded with iAs(V) sample towards lower wavenumber confirmed coordination of As towards C(=O)-O—. Thus, ATR-FTIR spectra revealed the adsorption mechanism of As on AC prepared from peanut shells.

Analyzing the subtracted spectra of Florisil®-AC loaded with iAs(V) at pH = 8, however, drastic spectral changes can be observed (Figure 13). The band at 1709 cm^{-1} belonging to C=O stretching (vC=O) of monodentate coordinated COO⁻ disappeared. The strong bands at 1070 and 1040 cm^{-1} can be assigned to C-OH groups, while the band at 791 cm^{-1} belongs to Si-OH vibration. This latter outcome also suggests that the hydroxyl groups of Florisil® bind the carboxylic groups of the AC more efficiently, rendering a mechanically stable granular presentation less prone to diffusion. However, this stronger binding is unfavorable to As adsorption.

By loading iAs(V) between 50 and 800 mg/L with the most promising AC varieties, As removal rate was approximately 20%, on average (Figure 12). Taking into account that the total immobilization rate of the AC expressed as the As concentration in the residual fraction was about 30–40% depending on the AC variety used (Figure 10a), from which the As immobilization rate by the soil itself artificially contaminated with iAs(V) was about 20%, the results obtained by loading ACs with iAs(V) solutions in varying concentrations and the immobilization studied conducted on soils were in good agreement.
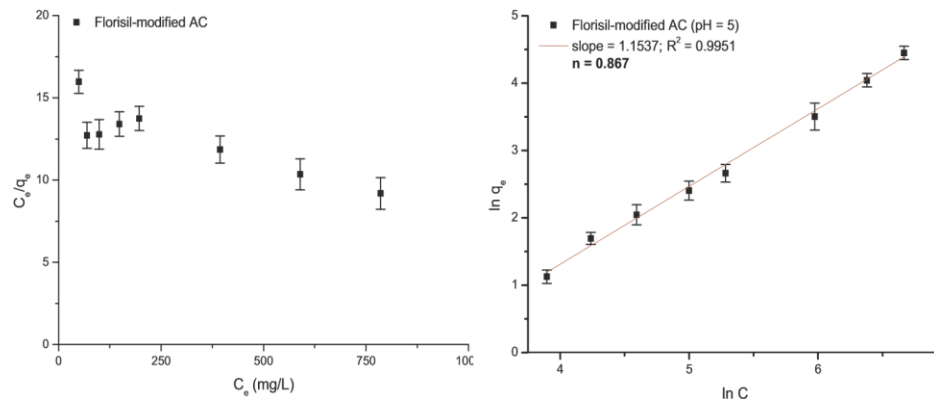
a)
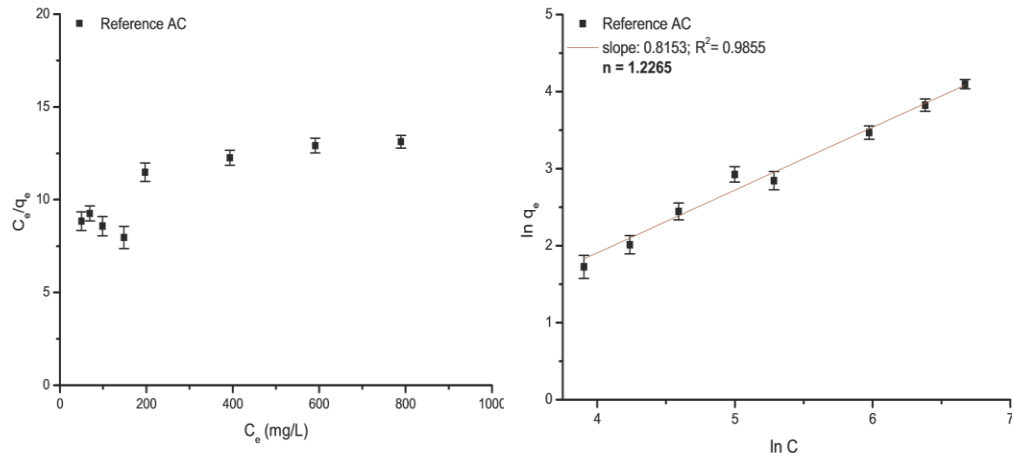
b)
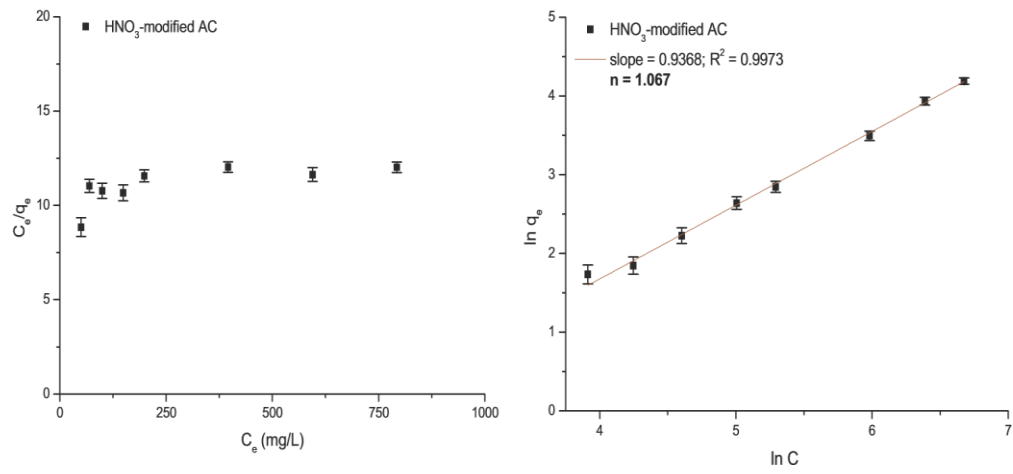
c)

Figure 12 a-c. Application of Langmuir and Freundlich isotherms for the experimentally determined data using reference (a), HNO$_3$-modified (b) and Florisil®-modified activated charcoal (AC) (c) at pH =5
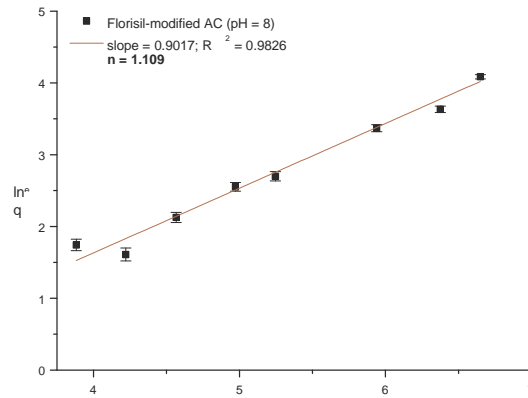
d)

Figure 12d. Application of Langmuir and Freundlich isotherms for the experimentally determined data using Florisil®-modified AC at pH =8 (d). Error bars represent the standard deviation of the results (n= 3)
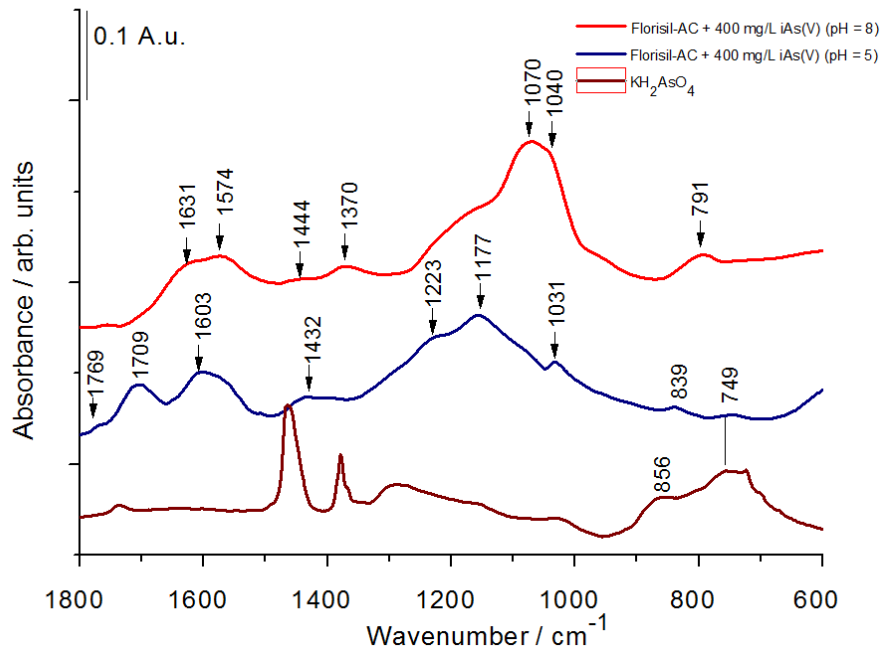

Figure 13. ATR-FT-IR spectrum of granular activated charcoal (AC) modified with florisil and loaded with 400mg/L iAs(V) at pH =5 (blue line) and 8 (red line) after spectral subtraction of the pure AC matrix one. A spectrum of KH_2AsO_4 brown line) has also been added.

6. Limitations of practical applications

These investigations were conducted on iAs(V) and iCr(III) mobility reduction in soils containing low OM content and were slightly contaminated with iAs(V). However, natural soil system contains different amounts of minerals, OM, CEC, etc. and these are vital in elements mobility. Therefore, to generalize the mobility reduction obtained in these experiments to other soils especially soils with higher As contamination and/or higher OM content could be considered biased. Since samples used in these experiments were either acidic or basic and so we are confident to assume that, soil with closely related pH values as used in these experiments would yield similar or better immobilization rates. Additionally, these experiments were performed in a laboratory setting with controlled experimental conditions (e.g. temperature, RH and artificial illumination) which are different from open environmental conditions. Therefore, these results cannot be directly extrapolated to real field investigations. Metal contamination occurs gradually in a long timeframe allowing the polluted soil to adjust and immobilize the contaminants overtime. However, in the case of these experiments, As and Cr were added at once. The concentration might have been too high for the soil to bind and incorporate in order to immobilize. Also, in natural soil system, several elements of various concentrations are also in the soil system and can influence the metal/metalloid mobility in it. To compare these findings to results with much higher or lower coexisting elements will give biased outcomes. The natural stabilizing agent (lignite or brown coal) from Hungary was used in this experiment which definitely could have different physical and chemical compositions to brown coal from other countries and so to conclude that the same application rates of brown coal of different, types and enrichment of varied functional groups would yield the same results could be untrue.

7. Summary

Mobility reduction capacity of 5 wt% lignite added in three particle size ranges (<0.5; 0.5–1.0 and 1.0–2.0 mm) to acidic (pH = 5.0) or calcareous (pH = 7.7) sandy soil samples of <2 mm grain size artificially contaminated with 375 mg/kg Cr(III) was assessed through fit-for-purpose leaching tests performed with CH_3COOH, $NH_2OH \cdot HCl$ and EDTA. About 90% and 60% of Cr(III) was immobilized in calcareous and acidic soils *per se*, respectively. Although the point of zero charge measurements ($pH_{pZC} \approx 4.5$) indicated that lignite could effectively bind positively charged Cr hydroxo complexes at the pH of the calcareous soil, application of lignite is unnecessary due to the low solubility of these species. Even though the acidic soil mobilizes Cr, addition of lignite has been proven to stabilize it. The phytoavailable Cr fraction in the soils *per se* was about 10-25%. In spite of the mobilization of Cr by acidic soil, the phytoavailable Cr concentration decreased to about half when the lignite particle size was either 0.5–1.0 or 1.0–2.0 mm. Lignite was suitable for Cr immobilization in acidic soil in a close particle size range, ensuring the dispersibility needed to enhance efficient Cr transfer from the contaminated soil to the stabilizer.

The same acidic sandy soil artificially contaminated with 15 mg/kg As in form of arsenate ions [iAs(V)] corresponding to the permissible value in force in Hungary was incubated for 4 weeks after amendment with different peanut shell-derived activated charcoal (AC) materials at an application rate of 2 wt%. Composite formation with silicate materials and adsorption mechanism for As were confirmed by attenuated total-reflection Fourier-transform infrared spectroscopy. Moreover, 0.01 M oxalic acid (OA) was also applied to investigate further enhancement through protonation of iAs(V) and/or AC. The aforementioned fit-for-purpose BCR sequential soil extraction and phytoavailability procedures have also been applied in this case. The largest As mobility reduction (approx. 30%) compared to the reference soil treatment was obtained when granular Florisil®-AC was applied. Mobility reduction did not improve by using OA. A 5 wt% AC application rate for the Florisil® composite resulted in a similar As distribution to the 2 wt% one also at a 30 mg/kg iAs(V) dosage. Amounts of immobilized As increased almost proportionally with 5 wt% AC by doubling the iAs(V) dose. Similarly, studies conducted on solutions proved that As adsorption onto ACs was slightly exponential.

8. New Results

By applying i) a fit-for-purpose BCR sequential soil extraction procedure consisting of leaching of Cr from the water-soluble and carbonatic as well as the easily reducible fractions with acetic acid and hydroxyl amine, respectively; and ii) leaching with EDTA for assessment of Cr phytoavailability of an acidic (pH = 5.0) as well as a calcareous soil (pH = 7.7) each artificially contaminated with 375 mg/kg inorganic Cr(III) and incubated for 8 weeks with 5% by weight lignite applied in three particle size ranges (<0.5; 0.5–1.0 and 1.0–2.0 mm), the following statements as new results can be made:

1. Since about 90% and 60% of the initial Cr(III) dose were immobilized by the calcareous and acidic soils *per se*, respectively, and taking into consideration pH-driven hydrolysis of Cr(III), soil pH is the main determining factor in the immobilization of this HM species. The point of zero charge measurements revealed that the surface of lignite is negatively charged above pH ≈ 4.5 enhancing adsorption of Cr(III) ions, as well as its positively charged hydroxo complexes formed at slightly basic pH values (up to 9). However, application of lignite is unnecessary in the case of calcareous soils due to the low water solubility of these latter species.

2. Phytoavailable Cr fraction was about 10–25%. These low values might be attributed to kinetic hindrance of Cr(III)-EDTA complex formation. Since leaching with hydroxylamine can be considered to some extent as a phytoavailable test because several higher plants are able to uptake nutrients through root surface acidification often accompanied by H^+-mediated reduction, the results obtained by hydroxylamine and EDTA leaching were compared. The results obtained for Cr leaching by hydroxylamine confirmed those results obtained by leaching with EDTA the acidic sandy soils where application of lignite is also effective.

3. Lignite grain size applied in the range of <0.5–2.0 mm in the present study did not provide any considerable additional gain on immobilization rates of Cr(III).

4. Arsenic adsorption onto ACs from iAs(V) model solutions proved to be adequately fitted with the Freundlich isotherm and adsorption was almost linear. Moreover, approximately 20% of the

total iAs(V) could be adsorbed. The acidic sandy soil *per se* could retain ≈15% of either 15 mg/kg or 30 mg/kg iAs(V), while in the presence of Florisil®-AC this ratio increased to 35% independently of the iAs(V) treatment dose.

5. The similar As immobilization rates obtained for the reference AC, HNO₃-and Florisil®-modified ACs indicate that, Florisil® has a role in the mechanical stabilization of the AC. Composite formation with silicate materials were confirmed by attenuated total-reflection Fourier-transform infrared spectroscopy (ATR-FTIR).

6. Adsorption of As to the AC is achieved by formation of a covalent bond between iAs(V) and O of the carboxylic functional group of the AC with simultaneous elimination of a water molecule and formation of a mixed acid anhydride according to the following equation:

$$Res - COOH + H_2AsO_4^- \rightarrow Res - COO - HAsO_3^- + H_2O$$
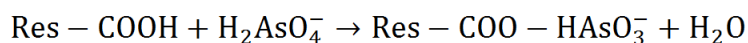
Coordination of As towards C(=O)-O— was confirmed by ATR-FTIR spectra.

7. By soaking the acidic soil with oxalic acid (OA) solution, the As mobility reduction rate did not further increase. Therefore, previously reported protonation of iAs(V) and/or biowaste derived AC with further enhancement possibility for As immobilization in soil by OA did not take place.

References

1. Rubinos, D. A., Spagnoli, G. (2019). Assessment of red mud as sorptive landfill liner for the retention of arsenic(V). J. Environ. Manage. 232, 271–285. doi:10.1016/j.jenvman.2018.09.041

2. Pigna, M., Caporale, A. G., Cavalca, L., Sommella, A., Violante, A. (2015). Arsenic in the Soil Environment: Mobility and Phytoavailability. Environ. Eng. Sci. 32, 551–563. doi:10.1089/ees.2015.0018

3. Beiyuan, J., Awad, Y.M., Beckers, F., Tsang, D.C.W., Ok, Y.S., Rinklebe, J. (2017). Mobility and phytoavailability of As and Pb in a contaminated soil using pine sawdust biochar under systematic change of redox conditions. Chemosphere 178, 110–118. doi: 10.1016/j.chemosphere.2017.03.022

4. Bhowmick, S., Pramanik, S., Singh, P.,Mondal, P., Chatterjee, D., Nriagu, J. (2018). Arsenic in groundwater of West Bengal, India: a review of human health risks and assessment of possible intervention options. Sci. Total Environ. 612, 148–169. doi: 10.1016/j.scitotenv.2017.08.216

5. Chakraborti, D., Rahman, M.M., Ahamed, S., Dutta, R.N., Pati, S., Mukherjee, S.C. (2016). Arsenic groundwater contamination and its health effects in Patna district (capital of Bihar) in the middle Ganga plain, In Magiera, T., Zawadzki, J., Szuszkiewicz, M., Fabijanczyk, P., Steinnes, E., Fabian, K., Miszczak, E., 2018. Impact of an iron mine and a nickel smelter at the Norwegian/Russian border close to the Barents Sea on surface soil magnetic susceptibility and content of potentially toxic elements. Chemosphere 195, 48-62. https://doi.org/10.1016/j.chemosphere.2017.12.060dia. Chemosphere 152, 520-529.

6. Mishra, S., Bharagava, R. N. (2015). Toxic and genotoxic effects of hexavalent chromium in environment and its bioremediation strategies. J. Environ. Sci. Heal C 34, 1–32. doi:10.1080/10590501.2015.1096883

7. Wuana, R.A., Okieimen, F.E. (2011). Heavy metals in contaminated soils: A review of sources, chemistry, risks and best available strategies for remediation. ISRN Ecology. 2011, 1–20. doi:10.5402/2011/402647

8. Dhal, B., Thatoi, H.N., Das, N.N., Pandey, B.D. (2013). Chemical and microbial remediation of hexavalent chromium from contaminated soil and mining/metallurgical solid waste: A review. J. Hazard. Mater. 250-251, 272–291. doi:10.1016/j.jhazmat.2013.01.048

9. Morillo, D., Pérez, G., Valiente, M. (2015). Efficient arsenic(V) and arsenic(III) removal from acidic solutions with Novel Forager Sponge-loaded superparamagnetic iron oxide nanoparticles, J. Colloid Interface Sci. 453, 132–141. doi:10.1016/j.jcis.2015.04.048

10. FAO and ITPS (2015). Status of the World's Soil Resources (SWSR)—technical summary Food and Agriculture Organization of the United Nations and Intergovernmental Technical Panel on Soils. Rome, Italy.

11. Mahmood-ul-Hassan, M., Suthar, V., Ahmad, R., Yousra, M. (2017). Heavy metal phytoextraction—natural and EDTA-assisted remediation of contaminated calcareous soils by sorghum and oat. Environ. Monit. Assess. 189, 591. doi:10.1007/s10661-017-6302-y

12. Derakhshan Nejad, Z., Jung, M.C., Kim, K.-H. (2017). Remediation of soils contaminated with heavy metals with an emphasis on immobilization technology. Environ. Geochem. Health, 40, 927–953. doi:10.1007/s10653-017-9964-z.

13. Janoš, P., Vávrová, J., Herzogová, L., Pilařová, V. (2010). Effects of inorganic and organic amendments on the mobility (leachability) of heavy metals in contaminated soil: A sequential extraction study. Geoderma 159, 335–41. doi:10.1016/j.geoderma.2010.08.009.

14. Klučaková, M., Omelka. L. (2004). Sorption of metal ions on lignite and humic acids. Chem. Pap. 58:170–75. doi: -

15. Godfray, H.C.J., Beddington, J.R., Crute, I.R., Haddad, L., Lawrence, D., Muir, J.F., Pretty, J., Robinson, S., Thomas, S.M., Toulmin, C. (2010). Food Security: The Challenge of Feeding 9 Billion People. Science, 327(5967), 812–818. doi:10.1126/science.1185383

16. Zhao, K., Liu, X., Xu, J., Selim, H.M. (2010). Heavy metal contaminations in a soil–rice system: Identification of spatial dependence in relation to soil properties of paddy fields. J. Hazard. Mater. 181, 778–787. doi:10.1016/j.jhazmat.2010.05.081.

17. Kaur, B., Singh, B., Kaur, N., Singh, D. (2017). Phytoremediation of cadmium-contaminated soil through multipurpose tree species. Agrofor. Sys. doi:10.1007/s10457-017-0141-2.

18. Bolan, N., Kunhikrishnan, A., Thangarajan, R., Kumpiene, J., Park, J., Makino, T., Kirkham, M.B., Scheckel, K. (2014). Remediation of heavy metal(loid)s contaminated soils - to mobilize or to immobilize? (Review). J. Hazard. Mater. 266, 141-166. doi:10.1016/j.jhazmat.2013.12.018.

19. Sanna, A., Uibu, M., Caramanna, G., Kuusik, R., Maroto-Valer, M.M. (2014). A review of mineral carbonation technologies to sequester CO_2. Chem. Soc. Rev., 43(23), 8049–8080. doi:10.1039/c4cs00035h.

20. Zhu, N., Yan, T., Qiao, J., Cao, H. (2016). Adsorption of arsenic, phosphorus and chromium by bismuth impregnated biochar: adsorption mechanism and depleted adsorbent utilization. Chemosphere 164, 32–40. doi:10.1016/j.chemosphere.2016.08.036.

21. Aydın, A.A., Aydın, A. (2014). Development of an immobilization process for heavy metal containing galvanic solid wastes by use of sodium silicate and sodium tetraborate. J. Hazard. Mater. 270, 35–44. doi:10.1016/j.jhazmat.2013.12.017

22. Szrek, D., Bajda, T., Manecki, M. (2011). A comparative study of the most effective amendment for Pb, Zn and Cd immobilization in contaminated soils. J. Environ. Sci. Heal. A 46, 1491–1502. doi:10.1080/10934529.2011.609082.

23. Huang, X., Muhammad, F., Yu, L., Jiao, B., Shiau, Y., Li, D. (2018). Reduction/immobilization of chromite ore processing residue using composite materials based geopolymer coupled with zero-valent iron. Ceram. Int. 44, 3454–3463. doi:10.1016/j.ceramint.2017.11.148.

24. Li, Y.C., Min, X.B., Chai, L.Y., Shi, M.Q., Tang, C.J., Wang, Q.W., Liang, Y.J., Lei, J., Liyang, W.J. (2016). Co-treatment of gypsum sludge and Pb/Zn smelting slag for the solidification of sludge containing arsenic and heavy metals. J. Environ. Manag. 181, 756–761. doi:10.1016/j.jenvman.2016.07.031.

25. Vondráčková, S., Hejcman, M., Tlustoš, P., Száková, J. (2013). Effect of quick lime and dolomite application on mobility of elements (Cd, Zn, Pb, As, Fe, and Mn) in contaminated soils. Pol. J. Environ. Stud. 22, (2), 577-589. doi: -

26. Yasuda, E.Y., Santos, R.G. dos, Vidal Trevisan, O. (2013). Kinetics of carbonate dissolution and its effects on the porosity and permeability of consolidated porous media. J. Petrol. Sci. Eng. 112, 284–289. doi:10.1016/j.petrol.2013.11.015.

27. Lim, J.E., Ahmad, M., Lee, S.S., Shope, C.L., Hashimoto, Y., Kim, K.-R., Usman, A.R.A., Yang, J.E., Ok, Y.S. (2013). Effects of lime-based waste materials on immobilization and phytoavailability of cadmium and lead in contaminated soil. CLEAN - Soil, Air, Water, 41(12), 1235–1241. doi:10.1002/clen.201200169.

28. Li, J.-S., Beiyuan, J., Tsang, D. C. W., Wang, L., Poon, C. S., Li, X.-D., Fendorf, S. (2017). Arsenic-containing soil from geogenic source in Hong Kong: Leaching characteristics and stabilization/solidification. Chemosphere. 182, 31–39. doi:10.1016/j.chemosphere.2017.05.019.

29. Milicevic, S., Boljanac, T., Martinovic, S., Vlahovic, M., Milosevic, V., Babic, B. (2012). Removal of copper from aqueous solutions by low cost adsorbent-Kolubara lignite. Fuel Process. Technol. 95, 1–7. DOI:10.1016/j.fuproc.2011.11.005.

30. Ghani, M.J., Rajoka, M.I., Akhtar, K. (2015). Investigations in fungal solubilization of coal: Mechanisms and significance. Biotechnol. Bioproc. E. 20, 634–642. doi:10.1007/s12257-015-0162-5.

31. Zhang, R., Wang, B., Ma, H. (2010). Studies on chromium(VI) adsorption on sulfonated lignite. Desalination. 255, 61–66. doi:10.1016/j.desal.2010.01.016.

32. Hori, M., Shozugawa, K., Matsuo, M. (2015). Reduction process of Cr(VI) by Fe(II) and humic acid analyzed using high time resolution XAFS analysis. J. Hazard. Mater. 285, 140–147. doi:10.1016/j.jhazmat.2014.11.047.

33. Zhao, T.T., Ge, W.Z., Yue, F., Wang, Y.X., Pedersen, C.M., Zeng, F.G., Qiao, Y. (2016). Mechanism study of Cr(III) immobilization in the process of Cr(VI) removal by Huolinhe lignite. Fuel Process. Technol. 152, 375–380. doi:10.1016/j.fuproc.2016.06.037.

34. Aldmour, S.T., Burke, I.T., Bray, A.W., Baker, D.L., Ross, A.B., Gill, F.L., Cibin, G., Ries, M.E., Stewart, D.I. (2018). Abiotic reduction of Cr(VI) by humic acids derived from peat and lignite: kinetics and removal mechanism. Environ. Sci. Pollut. Res. 26, 4717–4729. doi:10.1007/s11356-018-3902-1.

35. Guan, X., Dong, H., Ma, J. (2011). Influence of phosphate, humic acid and silicate on the transformation of chromate by Fe(II) under suboxic conditions. Sep. Purif. Technol. 78, 253–260. doi:10.1016/j.seppur.2011.02.031.

36. Jiang, W., Cai, Q., Xu, W., Yang, M., Cai, Y., Dionysiou, D. D., & O'Shea, K. E. (2014). Cr(VI) adsorption and reduction by humic acid coated on magnetite. Environ. Sci. Technol. 48, 8078–8085. doi:10.1021/es405804m.

37. Doskočil, L., Pekař, M. (2012). Removal of metal ions from multi-component mixture using natural lignite. Fuel Process. Technol. 101, 29–34. doi:10.1016/j.fuproc.2012.02.010.

38. Ding, W., Stewart, D.I., Humphreys, P.N., Rout, S.P., Burke, I.T. (2016). Role of an organic carbon-rich soil and Fe(III) reduction in reducing the toxicity and environmental mobility of chromium(VI) at a COPR disposal site. Sci. total. Environ. 541, 1191–1199. doi:10.1016/j.scitotenv.2015.09.150.

39. Leśniewska, B., Gontarska, M., Godlewska-Żyłkiewicz, B. (2017). Selective separation of chromium species from soils by single-step extraction methods: A critical appraisal. Water Air Soil Pollut. 228, 274. doi:10.1007/s11270-017-3459-5.

40. Chen, Z.-F., Zhao, Y.-S., Zhang, J.-W., Bai, J. (2015). Mechanism and kinetics of hexavalent chromium chemical reduction with sugarcane molasses. Water Air Soil Pollut. 226. 363. doi:10.1007/s11270-015-2629-6.

42. Oh, K., Cao, T., Li, T., Cheng, H. (2014). Study on application of phytoremediation technology in management and remediation of contaminated soils. J. Clean Energy. Technol. 2:216–220. doi:10.7763/JOCET.2014.V2.126.

43. Kohler, J., Caravaca, F., Azcón, R., Díaz, G., Roldán, A. (2015). The combination of compost addition and arbuscular mycorrhizal inoculation produced positive and synergistic effects on the phytomanagement of a semiarid mine tailing. Sci. Total Environ. 514, 42–48. doi:10.1016/j.scitotenv.2015.01.085.

44. Laghlimi M., Baghdad B., El Hadi, H., Bouabdli, A. (2015). Phytoremediation mechanisms of heavy metal contaminated soils: a review. Open J. Ecol. 5, 375–388. doi:10.4236/oje.2015.58031.

45. Gupta, P., Rani, R., Chandra, A., Varjani, S. J., Kumar, V. (2017). Effectiveness of plant growth-promoting rhizobacteria in phytoremediation of chromium stressed soils. Waste Bioremediation 301–312. doi:10.1007/978-981-10-7413-4_16.

46. Bian, F., Zhong, Z., Zhang, X., Yang, C. (2017). Phytoremediation potential of moso bamboo (Phyllostachys pubescens) intercropped with *Sedum plumbizincicola* in metal-contaminated soil. Environ. Sci. Pollut. Res. 24, 27244–27253. doi:10.1007/s11356-017-0326-2.

47. Ahmad, A., Hadi, F., Ali, N. (2014). Effective phytoextraction of cadmium (Cd) with increasing concentration of total phenolics and free proline in *Cannabis sativa* (L) plant under various treatments of fertilizers, plant growth regulators and sodium salt. Int. J. Phytoremediat. 17, 56–65. doi:10.1080/15226514.2013.828018.

48. Sallah-Ud-Din, R., Farid, M., Saeed, R., Ali, S., Rizwan, M., Tauqeer, H.M., Bukhari, S.A.H. (2017). Citric acid enhanced the antioxidant defense system and chromium uptake by *Lemna minor* L. grown in hydroponics under Cr stress. Environ. Sci. Pollut. Res. 24, 17669–17678. doi:10.1007/s11356-017-9290-0.

49. Lotfy, S.M., Mostafa, A.Z. (2014). Phytoremediation of contaminated soil with cobalt and chromium. J. Geochem. Explor. 144, 367–373. doi:10.1016/j.gexplo.2013.07.003.

50. Saravanan, A., Jayasree, R., Hemavathy, R.V., Jeevanantham, S., Hamsini, S., Senthil Kumar, P., Yaashikaa, P.R., Manivasagan, V., Yuvaraj, D. (2019). Phytoremediation of Cr(VI) ion contaminated soil using Black gram (*Vigna mungo*): Assessment of removal capacity. J. Environ. Chem. Eng. 103052. doi:10.1016/j.jece.2019.103052.

51. Singh, S., Parihar, P., Singh, R., Singh, V.P., Prasad, S.M. (2016). Heavy metal tolerance in plants: Role of transcriptomics, proteomics, metabolomics, and ionomics. Front. Plant Sci. 6:1143. doi: 10.3389/fpls.2015.01143.

53. Chen, Z., Wang, Y.P., Xia, D., Jiang, X., Fu, D., Shen, L., Wang, H., Li, Q.B. (2016). Enhanced bioreduction of iron and arsenic in sediment by biochar amendment influencing microbial community composition and dissolved organic matter content and composition. J. Hazard. Mater. 311: 20–29. doi:10.1016/j.jhazmat.2016.02.069.

54. Hussain, I., Li, M., Zhang, Y., Li, Y., Huang, S., Du, X., Liu, G., Hayat, W., Anwar, N. (2017). Insights into the mechanism of persulfate activation with nZVI/BC nanocomposite for the degradation of nonylphenol. Chem. Eng. 311, 163–172. doi:10.1016/j.cej.2016.11.085.

55. Harikishore Kumar Reddy, D., Lee, S.-M. (2014). Magnetic biochar composite: Facile synthesis, characterization, and application for heavy metal removal. Colloid. Surf. A: Physicochem. Eng. Asp. 454, 96–103. doi:10.1016/j.colsurfa.2014.03.105

56. Li, H., Dong, X., da Silva, E.B., de Oliveira, L.M., Chen, Y., Ma, L.Q. (2017). Mechanisms of metal sorption by biochars: Biochar characteristics and modifications. Chemosphere. 178, 466–478. doi:10.1016/j.chemosphere.2017.03.072.

57. Zhang, F., Wang, X., Xionghui, J., Ma, L. (2016). Efficient arsenate removal by magnetite-modified water hyacinth biochar. Environ. Pollut. 216, 575–583. doi:10.1016/j.envpol.2016.06.013.

58. Xu, Y., Fang, Z. (2015). The research progress of remediating the heavy metal-contaminated soil with biochar, Chin. J. Environ Eng. 35, 156-159. doi: -

59. Bian, R., Joseph, S., Cui, L., Pan, G., Li, L., Liu, X., Zhang, A., Rutlidge, H., Wong, S., Chia, C., Marjo, C., Bin Gong, B., Munro, P., Donne, S. (2014). A three-year experiment confirms continuous immobilization of cadmium and lead in contaminated paddy field with biochar amendment. J. Hazard. Mater. 272, 121–128. doi:10.1016/j.jhazmat.2014.03.017

60. Herath, I., Iqbal, M.C.M., Al-Wabel, M.I., Abduljabbar, A., Ahmad, M., Usman, A.R.A., Ok, Y.S., Vithanage, M. (2015). Bioenergy-derived waste biochar for reducing mobility, bioavailability, and phytotoxicity of chromium in anthropized tannery soil. J. Soil Sediment. 17, 731–740. doi:10.1007/s11368-015-1332-y.

61. Beesley, L., Moreno-Jiménez, E., Gomez-Eyles, J.L., Harris, E., Robinson, B., Sizmur, T. (2011). A review of biochars' potential role in the remediation, revegetation and restoration of contaminated soils. Environ. Pollut. 159, 3269–3282. doi:10.1016/j.envpol.2011.07.023.

62. Mohan, D., Pittman, C.U. (2007). Arsenic removal from water/wastewater using adsorbents—A critical review. J. Hazard. Mater. 142, 1–53. doi: 10.1016/j.jhazmat.2007.01.006. DOI:10.1016/j.jhazmat.2007.01.006.

63. Dias, J.M., Alvim-Ferraz, M.C., Almeida, M.F., Rivera-Utrillo, J., Sánchez-Polo, M. (2007). Waste materials for activated carbon preparation and its use in aqueous-phase treatment: a review, J. Environ. Manag. 85, 833–846. doi:10. 1016/j.jenvman.2007.07.031.

64. He, R., Peng, Z., Lyu, H., Huang, H., Nan, Q., Tang, J. (2018). Synthesis and characterization of an iron-impregnated biochar for aqueous arsenic removal. Sci. Total Environ. 612, 1177–1186. doi:10.1016/j.scitotenv.2017.09.016.

65. Trakal, L., Michálková, Z., Beesley, L., Vítková, M., Ouředníček, P., Barceló, A.P., Ettler, V., Číhalová, S., Komárek, M. (2018). AMOchar: amorphous manganese oxide coating of biochar improves its efficiency at removing metal(loid)s from aqueous solutions. Sci Total Environ. 625:71–78. doi:10.1016/j.scitotenv.2017.12.267.

66. Liang, J., Yang, Z., Tang, L., Zeng, G., Yu, M., Li, X., Wu. H., Qian. Y., Zeng. G., Luo, Y. (2017). Changes in heavy metal mobility and availability from contaminated wetland soil remediated with combined biochar-compost. Chemosphere. 181, 281–288. doi:10.1016/j.chemosphere.2017.04.081.

67. Wang, X., Yu, H.-Y., Li, F., Liu, T., Wu, W., Liu, C., Liu. C., Zhang, X. (2019). Enhanced immobilization of arsenic and cadmium in a paddy soil by combined applications of woody peat and $Fe(NO_3)_3$: Possible mechanisms and environmental implications. Sci. Total Environ. 649, 535–543. doi:10.1016/j.scitotenv.2018.08.387.

68. Gao, J., Lv, J.,Wu, H., Dai, Y., Nasir, M. (2018). Impacts of wheat straw addition on dissolved organic matter characteristics in cadmium-contaminated soils: insights from fluorescence spectroscopy and environmental implications. Chemosphere 193, 1027–1035. doi: 10.1016/j.chemosphere.2017.11.112.

69. Karami, N., Clemente, R., Moreno-Jiménez, E., Lepp, N.W., Beesley, L. (2011). Efficiency of green waste compost and biochar soil amendments for reducing lead and copper mobility and uptake to ryegrass. J. Hazard. Mater. 191, 41–48. doi:10.1016/j.jhazmat.2011.04.025.

70. Tang, W.W., Zeng, G.M., Gong, J.L., Liang, J., Xu, P., Zhang, C., Huang, B.B. (2014). Impact of humic/fulvic acid on the removal of heavy metals from aqueous solutions using nanomaterials: a review. Sci. Total Environ. 468, 1014–1027. DOI:10.1016/j.scitotenv.2013.09.044.

71. Tang, X., Li, X., Liu, X., Hashmi, M.Z., Xu, J., Brookes, P.C. (2015). Effects of inorganic and organic amendments on the uptake of lead and trace elements by *Brassica chinensis* grown in an acidic red soil. Chemosphere 119, 177–183. DOI:10.1016/j.chemosphere.2014.05.081.

72. Caporale, A.G., Pigna, M., Sommella, A., Dynes, J.J., Cozzolino, V., Violante, A. (2013). Influence of compost on the mobility of arsenic in soil and its uptake by bean plants (*Phaseolus vulgaris* L.) irrigated with arsenite-contaminated water. J. Environ. Manage. 128, 837. doi:10.1016/j.jenvman.2013.06.041.

73. Karna, R. R., Luxton, T., Bronstein, K. E., Hoponick Redmon, J., Scheckel, K. G. (2016). State of the science review: Potential for beneficial use of waste by-products for in situ remediation of metal-contaminated soil and sediment. Critical Reviews in Environmental Science and Technology, 47(2), 65–129. doi:10.1080/10643389.2016.1275417

74. Mikutta, R., Lorenz, D., Guggenberger, G., Haumaier, L., Freund, A. (2014). Properties and reactivity of Fe-organic matter associations formed by coprecipitation versus adsorption:

clues from arsenate batch adsorption. Geochim. Cosmochim. Acta 144, 258–276. doi:10.1016/j.gca.2014.08.026.

75. Chen, C.M., Dynes, J.J., Wang, J., Sparks, D.L. (2014). Properties of Fe-organic matter associations via coprecipitation versus adsorption. Environ. Sci. Technol. 48, 13751–13759. doi:10.1021/es503669u.

76. Huang, M., Zhu, Y., Li, Z., Huang, B., Luo, N., Liu, C., Zeng, G. (2016). Compost as a soil amendment to remediate heavy metal-contaminated agricultural soil: Mechanisms, efficacy, problems, and strategies. Water Air Soil Pollut. 227:359. doi:10.1007/s11270-016-3068-8.

77. Liang, J., Yang, Z., Tang, L., Zeng, G., Yu, M., Li, X., Wu. H., Qian. Y., Zeng. G., Luo, Y. (2017). Changes in heavy metal mobility and availability from contaminated wetland soil remediated with combined biochar-compost. Chemosphere. 181, 281–288. doi:10.1016/j.chemosphere.2017.04.081.

78. Guedes, P., Mateus, E. P., Couto, N., Rodríguez, Y., Ribeiro, A. B. (2014). Electrokinetic remediation of six emerging organic contaminants from soil. Chemosphere 117, 124–131. doi:10.1016/j.chemosphere.2014.06.017.

79. Mao, X., Han, F. X., Shao, X., Guo, K., McComb, J., Arslan, Z., Zhang, Z. (2016). Electro-kinetic remediation coupled with phytoremediation to remove lead, arsenic and cesium from contaminated paddy soil. Ecotoxicol. Environ. Saf. 125, 16–24. doi:10.1016/j.ecoenv.2015.11.021.

80. Wang, H., Song, H., Yu, R., Cao, X., Fang, Z., Li, X. (2016). New process for copper migration by bioelectricity generation in soil microbial fuel cells. Environ. Sci. Pollut. Res. 23, 13147–13154. doi:10.1007/s11356-016-6477-8.

81. Vocciante, M., Caretta, A., Bua, L., Bagatin, R., Ferro, S. (2016). Enhancements in ElectroKinetic Remediation Technology: Environmental assessment in comparison with other configurations and consolidated solutions. Chem. Eng. 289, 123–134. doi:10.1016/j.cej.2015.12.065.

82. Cameselle, C., Reddy, K.R. (2012). Development and enhancement of electro-osmotic flow for the removal of contaminants from soils. Electrochim. Acta 86, 10–22. doi:10.1016/j.electacta.2012.06.121.

83. de la Fuente, C., Clemente, R., Martínez-Alcalá, I., Tortosa, G., Bernal, M.P. (2011). Impact of fresh and composted solid olive husk and their water-soluble fractions on soil heavy metal

fractionation, microbial biomass and plant uptake. J. Hazard. Mater. 186, 1283–1289. doi:10.1016/j.jhazmat.2010.12.004.

84. Ryu, S. R., Jeon, E. K., Baek, K. (2017). A combination of reducing and chelating agents for electrolyte conditioning in electrokinetic remediation of As-contaminated soil. J. Taiwan Inst. Chem. E. 70, 252–259. doi:10.1016/j.jtice.2016.10.058.

85. Han, X., Wang, Y.F., Tang, X.K., Ren, H.T., Wu, S.H., Jia, S.Y. (2016). Lepidocrocite catalyzed Mn(II) oxygenation by air and its effect on the oxidation and mobilization of As(III). Appl. Geochem 72, 34-41. doi:10.1016/j.apgeochem.2016.06.009.

86. Lan, S., Wang, X., Xiang, Q., Yin, H., Tan, W., Qiu, G., Liu, F., Zhang, J., Feng, X. (2017). Mechanisms of Mn(II) catalytic oxidation on ferrihydrite surfaces and the formation of manganese (oxyhydr)oxides. Geochim. Cosmochim. Acta 211, 79-96. doi:10.1016/j.gca.2017.04.044.

87. Wei, X., Guo, S., Wu, B., Li, F., Li, G. (2015). Effects of reducing agent and approaching anodes on chromium removal in electrokinetic soil remediation. Front. Env. Sci. Eng. 10, 253–261. doi:10.1007/s11783-015-0791-0.

88. Fedje, K.K., Yillin, L., Strömvall, A.M. (2013). Remediation of metal polluted hotspot areas through enhanced soil washing – Evaluation of leaching methods. J. Environ. Manage. 128, 489–496. doi:10.1016/j.jenvman.2013.05.056.

89. Almaroai, Y.A., Usman, A.R.A., Ahmad, M., Kim, K.R., Vithanage, M., Ok, Y.S. (2013). Role of chelating agents on release kinetics of metals and their uptake by maize from chromated copper arsenate-contaminated soil. Environ. Technol. 34, 747–755. doi:10.1080/09593330.2012.715757.

90. Luo, C., Wang, S., Wang, Y., Yang, R., Zhang, G., Shen, Z. (2015). Effects of EDDS and plant growth- promoting bacteria on plant uptake of trace metals and PCBs from e-waste contaminated soil. J. Hazard. Mater. 286, 379–385. doi:10.1016/j.jhazmat.2015.01.010.

91. Kim, E.J., Lee, J.C., Baek, K. (2015). Abiotic reductive extraction of arsenic from contaminated soils enhanced by complexation: Arsenic extraction by reducing agents and combination of reducing and chelating agents. J. Hazard. Mater. 283, 454–461. doi:10.1016/j.jhazmat.2014.09.055.

92. Ryu, S. R., Jeon, E. K., Baek, K. (2017). A combination of reducing and chelating agents for electrolyte conditioning in electrokinetic remediation of As-contaminated soil. J. Taiwan Inst. Chem. E. 70, 252–259. doi:10.1016/j.jtice.2016.10.058.

93. Beiyuan, J., Lau, A.Y.T., Tsang, D.C.W., Zhang, W., Kao, C.-M., Baek, K., Ok, Y.S., Li, X.-D. (2018). Chelant-enhanced washing of CCA-contaminated soil: Coupled with selective dissolution or soil stabilization. Sci. Total Environ. 612, 1463-1472. doi:10.1016/j.scitotenv.2017.09.015.

94. Tsang, D.C.W., Hartley, N.R. (2014). Metal distribution and spectroscopic analysis after soil washing with chelating agents and humic substances. Environ. Sci. Pollut. Res. 21, 3987–3995. doi:10.1007/s11356-013-2300-y.

95. Tsang, D.C.W., Olds, W.E., Weber, P.A., Yip, A.C.K. (2013). Soil stabilisation using AMD sludge, compost and lignite: TCLP leachability and continuous acid leaching. Chemosphere 93, 2839–2847. doi:10.1016/j.chemosphere.2013.09.097.

96. Tsang, D.C.W., Yip, A.C.K., Olds, W.E., Weber, P.A. (2014). Arsenic and copper stabilisation in a contaminated soil by coal fly ash and green waste compost. Environ. Sci. Pollut. Res. 21, 10194–10204. doi:10.1007/s11356-014-3032-3.

97. Kim, E.J., Jeon, E.K., Baek, K. (2016). Role of reducing agent in extraction of arsenic and heavy metals from soils by use of EDTA. Chemosphere 152, 274–283. doi:10.1016/j.chemosphere.2016.03.005.

98. Beiyuan, J., Li, J., Tsang, D.C.W.,Wang, L., Poon, C.S., Li, X.D., Fendorf, S. (2017). Fate of arsenic before and after chemical-enhanced washing of an arsenic-containing soil in Hong Kong. Sci. Total Environ. 599–600, 679–688. doi:10.1016/j.scitotenv.2017.04.208.

99. Kim, E.J., Lee, J.C., Baek, K. (2015). Abiotic reductive extraction of arsenic from contaminated soils enhanced by complexation: Arsenic extraction by reducing agents and combination of reducing and chelating agents. J. Hazard. Mater. 283, 454–461. doi:10.1016/j.jhazmat.2014.09.055.

100. Voglar, D., Lestan, D. (2013). Pilot-scale washing of Pb, Zn and Cd contaminated soil using EDTA and process water recycling. Chemosphere 91, 76–82. doi:10.1016/j.chemosphere.2012.12.016.

101.   Li, G., Yang, X., Liang, L., Guo, S. (2017). Evaluation of the potential redistribution of chromium fractionation in contaminated soil by citric acid/sodium citrate washing. Arab. J. Chem. 10, S539–S545. doi:10.1016/j.arabjc.2012.10.016.

102.   Bagherifam, S., Lakzian, A., Fotovat, A., Khorasani, R., & Komarneni, S. (2014). In situ stabilization of As and Sb with naturally occurring Mn, Al and Fe oxides in a calcareous soil: Bioaccessibility, bioavailability and speciation studies. J. Hazard. Mater. 273, 247–252. doi:10.1016/j.jhazmat.2014.03.054.

103.   Zhu, N., Qiao, J., Yan, T. (2018). Arsenic immobilization through regulated ferrolysis in paddy field amendment with bismuth impregnated biochar. Sci. total Environ. 648, 993-1001. DOI:10.1016/j.scitotenv.2018.08.200.

104.   Jiang, J., Dai, Z., Sun, R., Zhao, Z., Dong, Y., Hong, Z., Xu, R. (2017). Evaluation of ferrolysis in arsenate adsorption on the paddy soil derived from an Oxisol. Chemosphere 179, 232–241. doi:10.1016/j.chemosphere.2017.03.115.

105.   Yu, H.Y., Li, F.B., Liu, C.S., Huang, W., Liu, T.-X., Yu, W.-M. (2016). Iron redox cycling coupled to transformation and immobilization of heavy metals: implications for paddy rice safety in the red soil of South China. Adv. Agron. 137, 279–317. doi:10.1016/bs.agron.2015.12.006.

106.   Madeira, A.C., de Varennes, A., Abreu, M.M., Esteves, C., Magalhães, M.C.F. (2012). Tomato and parsley growth, arsenic uptake and translocation in a contaminated amended soil. J. Geochem. Explor. 123, 114–121. doi:10.1016/j.gexplo.2012.04.004.

107.   Farrow, E.M., Wang, J., Burken, J.G., Shi, H., Yan, W., Yang, J., Hua, B., Deng, B. (2015). Reducing arsenic accumulation in rice grain through iron oxide amendment. Ecotoxicol. Environ. Saf. 118, 55–61. doi:10.1016/j.ecoenv.2015.04.014.

108.   Bhandari, N., Reeder, R. J., & Strongin, D. R. (2011). Photoinduced oxidation of arsenite to arsenate on ferrihydrite. Environ. Sci. Technol. 45, 2783–2789. doi:10.1021/es103793y.

109.   Xu, Y., Xu, X., Hou, H., Zhang, J., Zhang, D., Qian, G. (2013). Moisture content-affected electrokinetic remediation of Cr(VI)-contaminated clay by a hydrocalumite barrier. Environ. Sci. Pollut. Res. 23, 6517–6523. DOI:10.1007/s11356-015-5685-y.

110.   Baragaño, D., Alonso, J., Gallego, J.R., Lobo, M.C., Gil-Díaz, M. (2019). Zero valent iron and goethite nanoparticles as new promising remediation techniques for As-polluted soils. Chemosphere. 124624. doi:10.1016/j.chemosphere.2019.124624.

111.   Naseri, E., Reyhanitabar, A., Oustan, S., Heydari, A.A., Alidokht, L. (2014). Optimization arsenic immobilization in a sandy loam soil using iron-based amendments by response surface methodology. Geoderma 232-234, 547–555. doi:10.1016/j.geoderma.2014.06.009.

112.   Gonçalves, J.R. (2016). The soil and groundwater remediation with zero valent iron nanoparticles. In: Procedia Engineering, pp. 1268-1275. doi:10.1016/j.proeng.2016.06.122.

113.   O'Carroll, D., Sleep, B., Krol, M., Boparai, H., Kocur, C. (2013). Nanoscale zero valent iron and bimetallic particles for contaminated site remediation. Adv. Water Resour. 51, 104-122. doi:10.1016/j.advwatres.2012.02.005.

114.   Su, H., Fang, Z., Tsang, P. E., Fang, J., Zhao, D. (2016). Stabilisation of nanoscale zero-valent iron with biochar for enhanced transport and in-situ remediation of hexavalent chromium in soil. Environ. Pollut. 214, 94–100. doi:10.1016/j.envpol.2016.03.072.

115.   Boparai, H.K., Joseph, M., O'Carroll, D.M. (2011). Kinetics and thermodynamics of cadmium ion removal by adsorption onto nano zerovalent iron particles. J. Hazard. Mater. 186, 458–465. doi:10.1016/j.jhazmat.2010.11.029.

116.   Zhu, S., Ho, S.-H., Huang, X., Wang, D., Yang, F., Wang, L., Wang, C., Cao, X., Ma, F. (2017). Magnetic nanoscale zerovalent iron assisted biochar: Interfacial chemical behaviors and heavy metals remediation performance. ACS Sustain. Chem. Eng. 5, 9673–9682. doi:10.1021/acssuschemeng.7b00542.

117.   Gil-Díaz, M., Rodríguez-Valdes, E., Alonso, J., Baragaño, D., Gallego, J.R., Lobo, M.C. (2019). Nanoremediation and long-term monitoring of brownfield soil highly polluted with as and Hg. Sci. Total Environ. 675, 165-175. DOI:10.1016/j.scitotenv.2019.04.183.

118.   Nielsen, S.S., Petersen, L.R., Kjeldsen, P., Jakobsen, R. (2011). Amendment of arsenic and chromium polluted soil from wood preservation by iron residues from water treatment. Chemosphere 84, 383–389. doi:10.1016/j. chemosphere.2011.03.069.

119.   Gil-Díaz, M., Alonso, J., Rodríguez-Valdes, E., Pinilla, P., Lobo, M.C. (2014). Reducing the mobility of arsenic in brownfield soil using stabilised zero-valent iron nanoparticles. J. Environ. Sci. Heal. - Part A Toxic/Hazardous Subst. Environ. Eng. 49, 1361-1369. doi:10.1080/10934529.2014.928248.

120.   Zhang, W., Zheng, J., Zheng, P., Tsang, D.C.W., Qiu, R. (2015). Sludge-derived biochar for arsenic(III) immobilization: Effects of solution chemistry on sorption behavior. J. Environ. Qual. 44, 1119. doi:10.2134/jeq2014.12.0536

121.   Zhang, W., Zheng, P., Zheng, J., Qiu, R. (2015). Atrazine immobilization on sludge derived biochar and the interactive influence of coexisting Pb(II) or Cr(VI) ions. Chemosphere 134, 438-445. doi:10.1016/ j.chemosphere.2015.05.011.

122.   Parlayici, S., Eskizeybek, V., Avcı, A., Pehlivan, E. (2015). Removal of chromium(VI) using activated carbon-supported-functionalized carbon nanotubes. J. Nanostructure Chem. 5, 255–263. doi:10.1007/s40097-015-0156-z.

123.   Sheoran, V., Sheoran, A.S., Poonia, P. (2016). Factors Affecting Phytoextraction: A Review. Pedosphere, 26(2), 148–166. doi:10.1016/s1002-0160(15)60032-7.

124.   Zhu, S., Huang, X., Wang, D., Wang, L., Ma, F. (2018). Enhanced hexavalent chromium removal performance and stabilization by magnetic iron nanoparticles assisted biochar in aqueous solution: Mechanisms and application potential. Chemosphere 207, 50–59. doi:10.1016/j.chemosphere.2018.05.046.

125.   Bhargava, A., Carmona, F. F., Bhargava, M., & Srivastava, S. (2012). Approaches for enhanced phytoextraction of heavy metals. J. Environ. Manag. 105, 103–120. doi:10.1016/j.jenvman.2012.04.002.

126.   Loganathan, P., Vigneswaran, S., Kandasamy, J. (2013). Enhanced removal of nitrate from water using surface modification of adsorbents – a review. J. Environ. Manag. 131, 363–374. doi:10.1016/j.jenvman.2013.09.034.

127.   Shi, R., Liu, Z., Li, Y., Jiang, T., Xu, M., Li, J., Xu, R. (2019). Mechanisms for increasing soil resistance to acidification by long-term manure application. Soil Till. Res.185, 77–84. doi:10.1016/j.still.2018.09.004.

128.   Shi, R., Li, J., Xu, R., Qian, W. (2016). Ameliorating effects of individual and combined application of biomass ash, bone meal and alkaline slag on acid soils. Soil Till. Res. 162, 41–45. doi:10.1016/j.still.2016.04.017.

129.   Yuan, J.H., Xu, R.K., Wang, N., Li, J.Y. (2011). Amendment of acid soils with crop residues and biochars. Pedosphere 21, 302–308. doi:10.1016/s1002-0160(11)60130-6.

130.   Dai, Z., Zhang, X., Tang, C., Muhammad, N., Wu, J., Brookes, P.C., Xu, J. (2017). Potential role of biochars in decreasing soil acidification - a critical review. Sci. Total Environ. 581, 601–611. doi: 10.1016/j.scitotenv.2016.12.169.

131.   Rajiv Gandhi, M., Meenakshi, S. (2013). Preparation of amino terminated polyamidoamine functionalized chitosan beads and its Cr(VI) uptake studies. Carbohydr. Polym. 91, 631–637. doi:10.1016/j.carbpol.2012.08.028.

132.   Gopalakannan, V., Viswanathan, N. (2015). Synthesis of magnetic alginate hybrid beads for efficient chromium(VI) removal. Int. J. Biol. Macromol. 72, 862–867. doi:10.1016/j.ijbiomac.2014.09.024.

133.   Barnie, S., Zhang, J., Wang, H., Yin, H., Chen, H. (2018). The influence of pH, co-existing ions, ionic strength, and temperature on the adsorption and reduction of hexavalent chromium by undissolved humic acid. Chemosphere 212, 209–218. doi:10.1016/j.chemosphere.2018.08.067.

134.   Inyang, M., Gao, B., Pullammanappallil, P., Ding, W., Zimmerman, A.R. (2010). Biochar from anaerobically digested sugarcane bagasse. Bioresour. Technol. 101, 8868–8872. doi:10.1016/j.biortech. 2010.06.088.

135.   Zhao, N., Wei, N., Li, J., Qiao, Z., Cui, J., He, F. (2005). Surface properties of chemically modified activated carbons for adsorption rate of Cr (VI). Chem. Eng. 115, 133–138. doi:10.1016/j.cej.2005.09.017.

136.   Lin, S. H., Juang, R.-S. (2009). Adsorption of phenol and its derivatives from water using synthetic resins and low-cost natural adsorbents: A review. J. Environ. Mamag. 90, 1336–1349. doi:10.1016/j.jenvman.2008.09.003.

137.   Yang, G.C.C., Yen, C.H. (2013). The use of different materials to form the intermediate layers of tubular carbon nanofibers/carbon/alumina composite membranes for removing pharmaceuticals from aqueous solutions. J. Membr. Sci. 425-426, 121–130. doi:10.1016/j.memsci.2012.09.011.

138.   Jones, D.L., Darrah, P.R. (1994). Role of root derived organic acids in the mobilization of nutrients from the rhizosphere. Plant Soil, 166, 247–257. doi:10.1007/BF00008338.

139.   Wei, W., Wang, Y., Wang, Z., Han, R., Li, S., Wei, Z., Zhang, Y. (2016). Stability of chloropyromorphite in ryegrass rhizosphere as affected by root-secreted low molecular weight organic acids. PloS one, 11, e0160628. doi:10.1371/journal.pone.0160628.

140. Uzinger, N., Rékási, M., Draskovits, E., Anton, A. (2013). Stabilization of Cr, Pb, and Zn in Soil Using Lignite. Soil Sediment Contam. 23, 270–286. doi:10.1080/15320383.2014.826620.

141. Cavaliere, C., Montone, C.M., Capriotti, A.L., La Barbera, G., Piovesana, S., Rotatori, M., Valentino, F., Laganà, A. (2018). Extraction of polycyclic aromatic hydrocarbons from polyhydroxyalkanoates before gas chromatography/mass spectrometry analysis. Talanta 188, 671–675. doi:10.1016/j.talanta.2018.06.038.

142. Falman, J.C., Fagnant-Sperati, C.S., Kossik, A.L., Boyle, D.S., Meschke, J.S. (2019). Evaluation of secondary concentration methods for poliovirus detection in wastewater. Food Environ Virol. 11, 20-31. doi: 10.1007/s12560-018-09364-y.

143. Rauret, G., López-Sánchez, J. F., Sahuquillo, A., Barahona, E., Lachica, M., Ure, A. M., Davidson, C. M., Gomez, A., Lück, D., Bacon, J. et al. (2000). Application of a modified BCR sequential extraction (three-step) procedure for the determination of extractable trace metal contents in a sewage sludge amended soil reference material (CRM 483), complemented by a three-year stability study of acetic acid and EDTA extractable metal content. J. Environ. Monit. 2, 228–33. doi:10.1039/b001496f.

144. Lakanen, E., Ervio, R. (1971). A comparison of eight extractants for the determination of plant available micronutrients in soils, Acta Agr. Fenn. 123, 223–232. doi: -.

145. European Committee for Standardization EN 13346. (2000). Characterization of sludges – Determination of trace elements and phosphorus – Aqua regia extraction methods. Brussels, Belgium: European Committee for Standardization (CEN).

146. Varga, M., ELAbadsa M., Tatár, E. Mihucz, V.G. (2019). Removal of selected pharmaceuticals from aqueous matrices with activated carbon under batch conditions. Microchem. J. 148:661–72. doi:10.1016/j.microc.2019.05.038.

147. Stavropoulos, G.G.,S. Korili, A., Sakellaropoulos, G. P. (1993). Porosity characteristics of lignite chars. Stud. Sci. Surf. Catal. 80, 599–605. doi: -.

148. Khan, M., Sarwar. A. (2007). Determination of points of zero charge of natural and treated adsorbents. Surf. Rev. Lett. 14, 461–69. doi:10.1142/S0218625X07009517.

149. Rao, R., Khan, M., Rehman, F. (2011). Batch and column studies for the removal of lead(II) ions from aqueous solution onto lignite. Adsorpt. Sci. Technol. 29:83–98. doi:10.1260/0263-6174.29.1.83.

150. Khan, M., Bhuto, S. (2012). Preparation and characterization of activated carbon from lignite coal by chemical activation and its application for lead removal from wastewater. IJCEES 3:28–39. doi: -.

151. Rai, D., Sass, B. M., Moore, D. A. (1987). Chromium(III) hydrolysis constants and solubility of chromium(III) hydroxide. Inorg. Chem. 26:345–49. doi:10.1021/ic00250a002.

152. Pukalchik, M., Panova, M., Karpukhin, M., Yakimenko, O., Kydralieva, K., Terekhova, V. (2018). Using humic products as amendments to restore Zn and Pb polluted soil: A case study using rapid screening phytotest endpoint. J. Soils Sediments 18:750–61. doi:10.1007/s11368-017-1841-y.

153. Mejia, J., Roden, E. E., Ginder-Vogel, M. (2016). Influence of oxygen and nitrate on Fe (hydr)oxide mineral transformation and soil microbial communities during redox cycling. Environ. Sci. Technol. 50, 3580–3588. doi:10.1021/acs.est.5b05519.

154. KvVM-EüM-FVM common order 6/2009. (2009). (IV. 14.) about the standard limits and measurement of contamination for the protection of underground water and geological medium. Magyar Közlöny 51: 14398–414.

155. Vithanage, M., Herath, I., Joseph, S., Bundschuh, J., Bolan, N., Ok, Y.S., Kirkham, M.B., Rinklebe, J. (2017). Interaction of arsenic with biochar in soil and water: A critical review. Carbon 113, 219–230. doi:10.1016/j.carbon.2016.11.032.

156. Matovic, D. (2011). Biochar as a viable carbon sequestration option: global and Canadian perspective, Energy 36, 2011–2016. doi:10.1016/j.energy.2010. 09.031.

157. Graetsch, H. (1994). Structural characteristics of opaline and microcrystalline silica minerals, Rev. Mineral. Geol. 29, 209–232. doi: -

158. Zhang, L., Lin, Q., Guo, X., Verpoort, F. (2011). Sorption behavior of Florisil for the removal of antimony ions from aqueous solutions, Water Sci. Technol. 63, 2114–2122. doi:10.2166/wst.2011.297.

159. Marschner, P. (1995). Mineral Nutrition of Higher Plants, second ed., Elsevier, Amsterdam. doi: -

160. Svehla, G. (1996). Vogel's Qualitative Inorganic Analysis, seventh ed., Pearson Education, Essex. doi: -

161. Glaser, B., Lehmann, J., Zech, W. (2002). Ameliorating physical and chemical properties of highly weathered soils in the tropics with charcoal - a review. Biol. Fert. Soils 35, 219–230. doi:10.1007/s00374-002-0466-4.

162. Dutton, M.V., Evans, C.S. (1996). Oxalate production by fungi: Its role in pathogenicity and ecology in the soil environment, Canadian J. Microbiol. 42, 881-895. doi:10.1139/m94-114.

163. Alozie, N., Heaney, N., Lin, C. (2018). Biochar immobilizes soil-borne arsenic but not cationic metals in the presence of low-molecular-weight organic acids, Sci. Total Environ. 630, 1188–1194. doi:10.1016/j.scitotenv.2018.02.319.

164. Toor, M., Jin, B. (2012). Adsorption characteristics, isotherm, kinetics, and diffusion of modified natural bentonite for removing diazo dye, Chem. Eng. J. 187 (2012) 79–88. doi:10.1016/j.cej.2012.01.089.

SCI publications constituting the basis of the present dissertation

Anemana, T., Óvári, M., Szegedi, Á., Uzinger, N., Rékási, M., Tatár, E., Yao, J., Streli, C., Záray. G., Mihucz, V.G. (2019). Optimization of Lignite Particle Size for Stabilization of Trivalent Chromium in Soils. Soil and Sediment Contamination: An International Journal, 1–20. doi:10.1080/15320383.2019.1703100.

Anemana, T., Óvári, M., Varga, M., Mihály, J., Uzinger, N., Rékási, M., Jun Yao, J., Tatár, E., Streli, C., Záray, G., Mihucz, V.G. (2019). Granular activated charcoal from peanut (Arachis hypogea) shell as a new candidate for stabilization of arsenic in soil. Microchemical Journal, 149, 104030. doi:10.1016/j.microc.2019.104030.

Acknowledgements

I. The data of the doctoral dissertation:

Name of the author: **Timothy Amangdam Anemana**

MTMT-identifier:

Title and subtitle of the doctoral dissertation: **Reduction of arsenate and inorganic trivalent chromium mobility in soils**

DOI-identifier[72]: 10.15476/ELTE.2020.048

Name of the doctoral school: Doctoral School of Environmental Sciences

Name of the doctoral programme: Environmental Chemistry Doctoral Programme

Name and scientific degree of the supervisors: Viktor Mihucz & Enikő Tatár; Chemistry (PhD)

Workplace of the supervisors: Department of Analytical Chemistry, Institute of Chemistry ELTE

II. Declarations

1. As the author of the doctoral dissertation,[73]

a) I agree to public disclosure of my doctoral dissertation after obtaining a doctoral degree in the storage of ELTE Digital Institutional Repository. I authorize the administrator of the Department of Doctoral, Habilitational and International Affairs of the Dean's Office of the Faculty of Science to upload the dissertation and the abstract to ELTE Digital Institutional Repository, and I authorize the administrator to fill all the declarations that are required in this procedure.

b) I request to defer public disclosure to the University Library and the ELTE Digital Institutional Repository until the date of announcement of the patent or protection. For details, see the attached application form;[74]

c) I request in case the doctoral dissertation contains qualified data pertaining to national security, to disclose the doctoral dissertation publicly to the University Library and the ELTE Digital Institutional Repository ensuing the lapse of the period of the qualification process.;[75]

d) I request to defer public disclosure to the University Library and the ELTE Digital Institutional Repository, in case there is a publishing contract concluded during the doctoral procedure or up until the award of the degree. However, the bibliographical data of the work

shall be accessible to the public. If the publication of the doctoral dissertation will not be carried out within a year from the award of the degree subject to the publishing contract, I agree to the public disclosure of the doctoral dissertation and abstract to the University Library and the ELTE Digital Institutional Repository.[76]
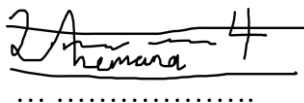
2. As the author of the doctoral dissertation, I declare that

a) the doctoral dissertation and abstract uploaded to the ELTE Digital Institutional Repository are entirely the result of my own intellectual work and as far as I know, I did not infringe anyone's intellectual property rights.;

b) the printed version of the doctoral dissertation and the abstract are identical with the doctoral dissertation files (texts and diagrams) submitted on electronic device.

3. As the author of the doctoral dissertation, I agree to the inspection of the dissertation and the abstract by uploading them to a plagiarism checker software.

Budapest, 2020 February the 28th

… ……………….

Signature of dissertation author

[72] *Filled by the administrator of the faculty offices.*

[73] *The relevant part shall be underlined.*

[74] *Submitting the doctoral dissertation to the Disciplinary Doctoral Council, the patent or protection application form and the request for deferment of public disclosure shall also be attached.*

[75] *Submitting the doctoral dissertation, the notarial deed pertaining to the qualified data shall also be attached.*

[76] *Submitting the doctoral dissertation, the publishing contract shall also be attached.*